

**Efficient Computation of Distribution Function
for Sum of Lognormal Random Variables &
Application to CDMA Data Network**

BY
ABDALLAH RASHED

A Thesis Presented to the
DEANSHIP OF GRADUATE STUDIES

KING FAHD UNIVERSITY OF PETROLEUM & MINERALS
DHAHRAN, SAUDI ARABIA

In Partial Fulfillment of the
Requirements for the Degree of

MASTER OF SCIENCE

In

COMPUTER ENGINEERING

December 2012



In the name of Allah, the Most Gracious and the

Most Merciful

KING FAHD UNIVERSITY OF PETROLEUM AND MINERALS

DHAHRAN 31261, SAUDI ARABIA

DEANSHIP OF GRADUATE STUDIES

This thesis, written by ABDALLAH RASHED under the direction of his thesis advisor and approved by his thesis committee, has been presented to and accepted by the Dean of Graduate Studies, in partial fulfillment of the requirements for the degree of **MASTER OF SCIENCE in COMPUTER ENGINEERING.**

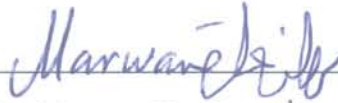
Thesis Committee



Dr. Ashraf S. Hasan Mahmoud (Advisor)



Dr. Lahouari Cheded (Member)



Dr. Marwan H. Abu-Amara (Member)



Dr. Basem AL-Madani
(Department Chairman)



Dr. Salam A. Zummo
(Dean of Graduate Studies)

Date

5 / 11 / 13



Dedicated

to

My Beloved Parents and Brothers

ACKNOWLEDGMENTS

All praise and thanks are due to Almighty Allah, Most Gracious and Most Merciful, for his immense beneficence and blessings. He bestowed upon me health, knowledge and patience to complete this work. May peace and blessings be upon prophet Muhammad (PBUH), his family and his companions.

Thereafter, acknowledgement is due to the support and facilities provided by the Computer Engineering Department of King Fahd University of Petroleum & Minerals for the completion of this work.

I acknowledge, with deep gratitude and appreciation, the inspiration, encouragement, valuable time and continuous guidance given to me by my thesis advisor, **Dr. Ashraf S. Hasan Mahmoud**. I am also grateful to my Committee members, **Dr. Lahouari Cheded** and **Dr. Marwan H. Abu-Amara** for their constructive guidance and support.

My heartfelt thanks are due to my parents and brothers for their prayers, guidance, and moral support throughout my academic life. My parents' advice, to strive for excellence has made all this work possible.

Last, but not least, thanks to all my colleagues and friends who encourage me a lot in my way to the achievement of this work.

TABLE OF CONTENTS

ACKNOWLEDGMENTS.....	IV
TABLE OF CONTENTS.....	V
LIST OF FIGURES	VII
LIST OF TABLES	X
ABBREVIATIONS	XI
THESIS ABSTRACT (ENGLISH).....	XII
THESIS ABSTRACT (ARABIC)	XIV
CHAPTER 1 INTRODUCTION.....	1
1.1 INTRODUCING THE PROBLEM AND THE IMPORTANCE OF THE SOLUTION	1
1.2 BACKGROUND.....	3
1.3 PROBLEM STATEMENT	13
1.4 THESIS CONTRIBUTIONS	14
CHAPTER 2 LITERATURE REVIEW.....	15
CHAPTER 3 METHODS OF ENHANCING THE COMPUTATIONS OF THE DISTRIBUTION FUNCTION OF LN RVS.....	22
3.1 USE OF OSCILLATORY QUADRATURES.....	22
3.2 USING QUADRATURES TO APPROXIMATE CDF OF SUM OF LN RVS.....	24
3.3 APPLICATION OF THE EPSILON ALGORITHM.....	26
3.4 NUMERICAL RESULTS AND DISCUSSION	28
CHAPTER 4 ANALYSIS AND IMPLEMENTATION OF LEGENDRE-GAUSS QUADRATURE ...	34
4.1 EVALUATION OF THE CF OF LN RV USING OPTIMIZED INTEGRAL LIMITS	35

4.2 EVALUATION OF THE CF OF LN RV USING FIXED INTEGRAL LIMITS	40
4.3 UTILIZATION OF LGQ WITH OPTIMIZED LIMIT IN COMPUTING CDF OF SUM OF INDEPENDENT LN RVs	48
CHAPTER 5 APPLICATION TO CDMA DATA NETWORK	50
5.1 BACKGROUND MATERIAL.....	50
5.2 PARAMETERIZATION OF THE DISTRIBUTION OF \mathbf{fk}	54
5.3 DEVELOPED EXPRESSIONS FOR $\mathbf{FB}(x)$ AND $\mathbf{FA}(x)$	58
5.4 NUMERICAL RESULTS	61
CHAPTER 6 CONCLUSION AND FUTURE DIRECTIONS	67
6.1 CONCLUSIONS.....	67
6.2 FUTURE DIRECTIONS.....	69
REFERENCES	71
VITA.....	79

LIST OF FIGURES

Figure 1.1: (a) PDF of Lognormal RV. (b) CDF of Lognormal RV.	7
Figure 1.2: CDF of the IID sum of lognormal RVs plotted on a normal probability scale with $\mu=0$ and $\sigma =12$ dB for various values of K [24].	13
Figure 3.1 The CDF of the sum of $K=20$ IID lognormal RVs $\mu_{dB}= 0$ dB and $\sigma_{dB} = 6$ dB and $\sigma_{dB}=12$ dB using the curve fit in [35] and three quadrature rules: Clenshaw-Curtis, Fejer2, and Legendre.	29
Figure 3.2 Sum of squared relative errors between CDF evaluated using quadrature rules and curve fit versus number of weights and nodes for sum of 20 IID LN RVs and $\sigma_{dB} = 12$ dB.	31
Figure 3.3 The CDF for the sum W evaluated using relation (3.10) for 20 IID LN RVs and σ_{dB} equal to 6 dB and 12 dB.	32
Figure 3.4 The CDF for the sum W evaluated using the Epsilon algorithm for 6 and 20 IID LN RVs and σ_{dB} equal 12 dB.	33
Figure 4.1: Evaluation of optimized integral limits for the cases of (a) $\sigma_{dB} = 6$ dB, and (b) $\sigma_{dB} = 12$ dB.	38
Figure 4.2: Evaluation of relative error for the computation of absolute of CF for $\sigma_{dB} = 12$ dB using HGQ and LGQ with optimized integral limits.	40

Figure 4.3: Evaluation of relative error for the computation of absolute of CF for $\sigma_{dB} = 12$ dB using HGQ and LGQ with fixed integral limits a^* and b^*42

Figure 4.4: Surface for logarithm of weighted sum of relative error for the computation of absolute CF for $\sigma_{dB} = 12$ dB using the LGQ rule with $N = 10$ as a function integral limits a and b46

Figure 4.5: Evaluation of relative error for the computation of absolute of CF for $\sigma_{dB} = 12$ dB using HGQ and LGQ with fixed integral limits a and b47

Figure 4.6: The CDF of the sum of $K=20$ IID lognormal RVs $\mu_{dB}= 0$ dB and $\sigma_{dB} = 6$ and 12 dB using the curve fit in [35] and three quadrature rules: Clenshaw-Curtis, Fejer2, and Legendre, with optimized integral limits a and b for LGQ approach.49

Figure 4.7: The CDF of the sum of $K=20$ IID lognormal RVs $\mu_{dB}= 0$ dB and $\sigma_{dB} = 6$ and 12 dB using the curve fit in [35] and three quadrature rules: Clenshaw-Curtis, Fejer2, and Legendre, with quasi-optimized integral limits a and b for LGQ approach.49

Figure 5.1: Cellular configuration for cell-site traffic power problem showing cell of interest, numbered cell 0, and cells belonging to first tier of co-channel interferers numbered 1 to 6. Cells belonging to second tier of co-channel interferers numbered 7 to 18 are not shown.52

Figure 5.2: Distribution function for RV f_k evaluated using Monte-Carlo simulations or using the new expression with $N = 5$ for different values of path loss exponent α and shadowing spread σ_{dB} . The simulation results are shown using markers while the new expression results are plotted as lines.57

Figure 5.3: CDF plots for RV $B = k = 0K - 1Gkfk$ for path loss exponent equal to 4 and two shadowing spread values (6 dB and 12 dB).....64

Figure 5.4: Probability of power outage for the four selected states: state 1 = (1, 0, 0, 0, 0), state 2 = (0, 0, 0, 0, 1), state 3 = (1, 1, 0, 1, 1), and state 4 (0, 2, 0, 1, 1).....65

Figure 5.5: Power outage probability as a function of number of connections for a specific mixture of connection rates for a path loss exponent of 4 and a shadowing spread of 6 dB and 12 dB.....66

LIST OF TABLES

Table 2.1: Seven Types of Pearson Distributions [38]	20
Table 3.1: The Epsilon algorithm table.....	28
Table 4.1: quasi-optimized integral limits for LGQ rule.	45
Table 5.1: Approximation for fk RV and parameters μ and σ for equivalent LN RV.....	58
Table 5.2: Simulation parameters used for WCDMA system.	62

Abbreviations

BW	Bandwidth
CC	Clenshaw-Curtis
CDF	Cumulative distribution function
CDMA	Code Division Multiple Access
CF	Characteristic Function
DS	Direct sequence
HGQ	Hermite-Gauss Quadrature
IID	Independent and Identically Distributed
INID	Independent but non Identically Distributed
LGQ	Legendre-Gauss Quadrature
LSG	Log-shifted gamma
LN	lognormal
MGFM	Moment Generating Function Matching
MMA	Moment Matching Approximation
MoMs	Method of Moments
PDF	Probability distribution function
RF	Radio frequency
RV(s)	Random variable(s)
SSRE	The sum of relative errors squared
UWB	Ultra-Wide Band
WSRE	The weighted sum of relative errors

THESIS ABSTRACT (ENGLISH)

NAME: ABDALLAH RASHED

TITLE: Efficient Computation of Distribution Function for Sum of Lognormal Random Variables and Application to CDMA Data Network

MAJOR FIELD: COMPUTER ENGINEERING

DATE OF DEGREE: SAFAR 1434 (H) (DEC 2012 G)

Characterizing the distribution of the sum of lognormal random variables (RVs) is still an open issue; it appears in a variety of fields and has been the target objective of many papers. In wireless communications, it arises in analyzing the total power received from several interfering sources. Recent advances in this field allow for the efficient computations of the distribution of a low number of individual RV components or for low value of the decibel spread corresponding to the individual RV. This work attempts to explore methods that are more efficient and easier in evaluating the distribution function for the sum of lognormal RVs. Previous research works in the area of wireless code-

division-multiple-access (CDMA) data networks have shown that the cell-site traffic power can be modeled as the sum of RVs that are very similar to lognormal RVs. This work also aims to apply the developed computation to the problem of characterizing the cell-site power for CDMA system.

MASTER OF SCIENCE DEGREE

KING FAHD UNIVERSITY OF PETROLEUM AND MINERALS

Dhahran, Saudi Arabia

THESIS ABSTRACT (ARABIC)

ملخص الرسالة

الاسم: عبدالله راشد

عنوان الرسالة: إيجاد دالة الكثافة الإحتمالية أو دالة التوزيع التراكمي لمجموع عدد من المتغيرات العشوائية اللوغارتمية وتطبيقها على نظام الشبكات اللاسلكية المعتمد على تقسيم الشيفرة.

التخصص: هندسة الحاسوب

تاريخ التخرج: صفر 1433 هـ - (كانون الأول 2012 م)

ما زالت مشكلة إيجاد دالة الكثافة الإحتمالية أو دالة التوزيع التراكمي لمجموع عدد من المتغيرات العشوائية اللوغارتمية مجال البحث فيها مفتوح ومتجدد، حيث تظهر هذه المعضلة في الكثير من المجالات العلمية المتعددة وتتصدر من حيث الأهمية العديد من المنشورات. على سبيل المثال، تظهر أهميتها جليا في الإتصالات اللاسلكية، من حيث تحليل مجموع القدرة الكهرومغناطيسية المكتسبة من تداخل عدة مصادر لهذه القدرة. هنالك أبحاث متقدمة حديثة في هذا المجال أوجدت طرق للحسابات المتعلقة لهذه المعضلة الرياضية بكفاءة إما لعدد معين قليل من المتغيرات العشوائية المستقلة أو لقيمة صغيرة للانحراف المعياري المتعلق بهذه المتغيرات. الدراسة في هذه الأطروحة

هي محاولة لإيجاد طرق أسهل وأكثر كفاءة لحساب دالة الكثافة الإحتمالية أو دالة التوزيع التراكمي لمجموع عدد من المتغيرات العشوائية اللوغارتمية. هنالك أبحاث سابقة في مجال الشبكات اللاسلكية، المعروفة بالإختصار (CDMA)، أثبتت أنّ دراسة مجموع القدرة الكهرومغناطيسية في الموقع الخلوي يمكن صياغتها بطريقة حسابية مشابهة لدراسة المتغيرات العشوائية اللوغارتمية. الدراسة في هذه الأطروحة أيضا سوف تهدف الى تطبيق الحسابات المبتكرة المتعلقة بهذه المتغيرات على مسألة دراسة حركة القدرة الكهرومغناطيسية في الموقع الخلوي و كيفية حسابها للنظام (CDMA).

شهادة ماجستير علوم

جامعة الملك فهد للبترول والمعادن

الظهران ، المملكة العربية السعودية

Chapter 1

INTRODUCTION

This chapter introduces the problem of characterizing the sum of lognormal random variables along with its importance in various scientific fields.

1.1 Introducing the Problem and the Importance of the Solution

The sum of lognormal distribution has no closed-form equation and is difficult to compute numerically. Several approximations have been proposed for it and employed in the literature, most, if not all, of these approaches are typically valid for very specific ranges of the parameters of the sum. The lognormal (LN) random variables (RVs) topic appears in a variety of scientific fields and has been studied in many papers [1-5]. It arises in wireless communications when analyzing the total power received from several interfering sources [6-8], and in fields such as physics [2], electronics [3], optics [9], economics [10], and it is also of interest to statistical mathematicians [11-12].

In the area of wireless or radio frequency (RF) engineering, the LN RV is used to model the signal level with large-scale variations due to obstacles and signal shadowing [13]. It is of great importance to characterize the sum of LN RVs in terms of the overall probability density function (PDF) or the cumulative distribution function (CDF). This

characterization may be used to quantify the probability of the sum exceeding or dropping below a certain threshold value.

The LN RV is specified by the parameters μ and σ , which are the mean and standard deviation, respectively, of the corresponding normal RV. A preferred characterization for the sum of the LN RVs would be in terms of the μ 's and σ 's of the individual LN RVs. Furthermore, the preferred characterization should present the final approximation in the form of an expression, or formula that is easy and convenient to evaluate, without relying on quantities that need to be evaluated empirically or on using nested numerical integrations.

Recent advances in the area of computing the distribution function for the sum of LN RVs, such as those in [14] and [15], have only allowed for the efficient computation of the distribution function for the sum, for specific cases of the general problem. Specifically, the study in [14] has produced new and relatively accurate simple expressions for the characteristic function for the sum of LN RVs. The work in this Master thesis aims to extend the utilization of these expressions and allow for more efficient calculations of the distribution of the sum.

In addition, previous research has shown that the cell-site transmitted traffic power for the wireless Code Division Multiple Access (CDMA) data network can be modeled as the sum of lognormal-like RVs. The work herein also aims to apply the developed methods to this problem as well.

1.2 Background

The background material is presented in two subsections. The first subsection, describes the lognormal random variable and its characterization while the second subsection defines the problem of the sum of the lognormal random variables. The second subsection also outlines the main results with respect to the problem of the sum of LN RVs that would be the basis for the work carried out in this thesis.

The background material required for the example application, i.e. the cell-site traffic power characterization problem for CDMA wireless data networks will be included in Chapter 5.

1.2.1 The Lognormal Random Variable

If X is a normal random variable with mean and standard deviation specified by μ_X and σ_X , respectively, then $Z = \exp(X)$ has a lognormal distribution. Conversely, if Z has a lognormal distribution, then $X = \ln(Z)$ is normally distributed. The PDF of X is given by:

$$f_X(x) = \frac{1}{\sqrt{2\pi} \sigma_X} \exp\left[-\frac{(x - \mu_X)^2}{2\sigma_X^2}\right], \quad x \in [-\infty, \infty] \quad (1.1)$$

then the PDF of Z can be consequently written in terms of the moments of X , as follows:

$$f_Z(z) = \begin{cases} \frac{1}{\sqrt{2\pi} \sigma_X z} \exp\left[-\frac{(\ln(z) - \mu_X)^2}{2\sigma_X^2}\right], & z > 0 \\ 0, & z \leq 0 \end{cases} \quad (1.2)$$

The moments of the lognormal RV Z can be evaluated by using the n^{th} moment generating function of the normal distribution as follows:

$$\begin{aligned} E[Z^n] &= E[(e^X)^n] \\ &= \int_{-\infty}^{\infty} e^{xn} \frac{1}{\sqrt{2\pi} \sigma_X} \exp\left[-\frac{(x - \mu_X)^2}{2\sigma_X^2}\right] dx \\ &= e^{n\mu_X + \frac{1}{2}n^2\sigma_X^2} \end{aligned} \quad (1.3)$$

For example, the mean of Z , $E[Z]$, is given by setting $n = 1$ in relation (1.3) to be

$$E[Z] = E[e^X] = e^{\mu_X + \frac{1}{2}\sigma_X^2} \quad (1.4)$$

while the variance is given by

$$\begin{aligned} \sigma_Z^2 &= E[Z^2] - (E[Z])^2 \\ &= e^{2\mu_X + \sigma_X^2} (e^{\sigma_X^2} - 1) \end{aligned} \quad (1.5)$$

The cumulative distribution function (CDF) of the lognormal RV Z , defined as $\text{Prob}(Z \leq z)$ is simply given by:

$$F_Z(z) = \Psi\left(\frac{\ln(z) - \mu_X}{\sigma_X}\right) \quad (1.6)$$

where $\text{Prob}(Z \leq z)$ is the probability that the RV Z is less than or equal to the value z and $\Psi(\cdot)$ is the CDF for the standard normal distribution with zero-mean and unit variance.

Moreover, in engineering fields, it is customary to represent the lognormal distribution in decibels as $Z = 10^{Y/10}$, where Y is a normal random variable with mean and standard deviation specified by μ_Y and σ_Y , respectively. Therefore, if Z has a lognormal distribution, then $Y = 10\log_{10}(Z)$ is normally distributed. The PDF of Z in terms of the moments of Y is specified by:

$$f_Z(z) = \begin{cases} \frac{1}{\zeta\sqrt{2\pi}\sigma_Y z} \exp\left[-\frac{(10\log_{10}(z) - \mu_Y)^2}{2\sigma_Y^2}\right], & z > 0 \\ 0, & z \leq 0 \end{cases} \quad (1.7)$$

where $\zeta = \frac{\ln(10)}{10} = 0.23026$ [16]. The RV X is related to the RV Y by the following relation:

$$Y = \frac{1}{\zeta} X. \quad (1.8)$$

as a result, the mean and standard deviation of Y are as following:

$$\mu_Y = \frac{1}{\zeta} \mu_X. \quad (1.9)$$

and

$$\sigma_Y = \frac{1}{y} \zeta \sigma_X. \quad (1.10)$$

In a mobile radio environment, the parameter $\sigma_Y = \frac{1}{\zeta} \sigma_X$ in decibels, sometimes called the decibel spread. It typically ranges between 6 dB and 12 dB for practical channels [17]. These ranges can be classified depending on the severity of the shadowing effect [8]. For example, 6 dB represents a light-shadowed mobile radio environment, while 12 dB represents a heavy-shadowed environment. In Ultra-Wide Band (UWB) transmission environments, the decibel spread takes on values that range between 3 dB and 5 dB [18]. However, it is more convenient to work with the natural logarithm as opposed to the decibel scale.

Let a lognormal RV Z be denoted by $\text{LN}(\mu, \sigma)$. The PDF and CDF curves for the single lognormal RV for various values of σ and $\mu = 0$, are shown in Figure 1.1: (a) and (b), respectively.

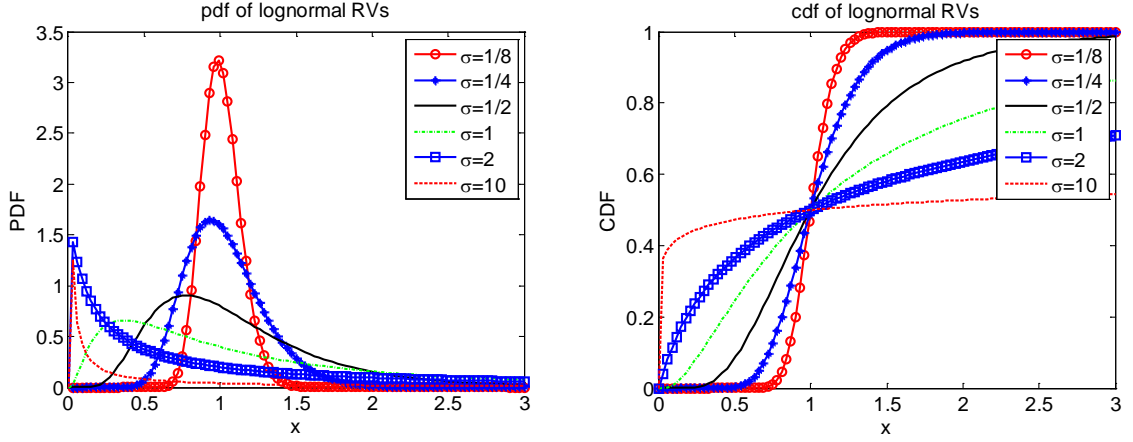


Figure 1.1: (a) PDF of Lognormal RV. (b) CDF of Lognormal RV.

The characteristic function (CF) for the lognormal RV Z $\Phi_Z(\omega)$ is defined using:

$$\Phi_Z(\omega) = \int_0^{\infty} e^{j\omega z} f_Z(z) dz \quad (1.11)$$

1.2.2 The sum of Lognormal Random Variables

Let W the sum of K LN RVs, be defined as the following:

$$W = Z_1 + Z_2 + \dots + Z_K = \sum_{k=1}^K Z_k \quad (1.12)$$

where the lognormal RV Z_k has the parameters μ_k and σ_k . The RVs Z_k 's can be either statistically independent or correlated. It is desired to compute the PDF $f_W(z)$ or CDF $F_W(z)$ of the RV W .

For the case of independent Z_k 's, the conventional method for computing the distribution of the sum is first to compute the individual CF' $\Phi_{Z_k}(\omega)$ for the lognormal RV' Z_k , and then the CF for the sum W would be simply the multiplication of the individual CF's as giving below:

$$\Phi_W(\omega) = \prod_{k=1}^K \Phi_{Z_k}(\omega) \quad (1.13)$$

For the case of independent and identically distributed (IID) Z_k 's, $\Phi_W(\omega)$ is given by:

$$\Phi_W(\omega) = [\Phi_Z(\omega)]^K \quad (1.14)$$

subsequently, the PDF for W may be obtained by the inverse Fourier transform specified by

$$f_W(z) = \int_{-\infty}^{\infty} e^{-j\omega z} \Phi_W(\omega) d\omega \quad (1.15)$$

The CDF for W can be obtained by either integrating $f_W(z)$ or directly from the corresponding CF using the relation developed in [19]:

$$F_W(z) = \frac{2}{\pi} \int_0^{\infty} \frac{\text{Re}\{\Phi_W(\omega)\}}{\omega} \sin(\omega z) d\omega \quad (1.16)$$

It can be seen from the previous material, that evaluating the CF $\Phi_{Z_k}(\omega)$ for the individual LN RV plays a major role in evaluating the required PDF or CDF for the sum of lognormal RVs W . Unfortunately, evaluating $\Phi_{Z_k}(\omega)$ is not an easy task, since the envelope for the integrand in (1.11) does not decay sufficiently fast. Rewriting the integrand in (1.11) in terms of the normal RV X PDF, results in an integrand that oscillates at an exponential frequency, due to the term $\exp(j\omega e^x)$. Therefore, the numerical evaluation of the CF as given by (1.11) requires the use of specialized numerical integration methods. Recently, Gubner [20] presented another form that is much easier to evaluate and which relies on reducing the oscillation in the integrand of (1.11), and employing the Hermite Gauss quadrature (HGQ) technique as the numerical integration method. The study in [15] generalizes Gubner's approach and proposes forms with almost no oscillations that result in more accurate evaluations of $\Phi_{Z_k}(\omega)$. Unfortunately, these new forms are non-parametric and involve nested calculations. The previous work in [14] relies on the result produced by Gubner [20] to write the approximate CF for the RV Z_k as follows:

$$\tilde{\Phi}_{Z_k}(\omega) = \sum_{n=1}^N A_n^{(k)} e^{-a_n^{(k)} \omega} \quad (1.17)$$

where the constants $A_n^{(k)}$ and $a_n^{(k)}$ are given in terms of the RV parameters μ_k and σ_k , and the first N -points of the HGQ weights and nodes. The superscript (k) indicates that the

constants are specific to the k^{th} lognormal RV only. The HGQ weights and nodes are identical for any N -points of HGQ and are typically tabulated as in [21]. By utilizing (1.13) and (1.14), the approximated CF for the sum of lognormal RVs W can be given by the following equation:

$$\tilde{\Phi}_W(\omega) = \prod_{k=1}^K \left[\sum_{n=1}^N A_n^{(k)} e^{-a_n^{(k)} \omega} \right] \quad (1.18)$$

for the independent but non identically distributed (INID) case. For the independent and identically distributed (IID) case, the approximate CF is given by:

$$\tilde{\Phi}_W(\omega) = \left[\sum_{n=1}^N A_n e^{-a_n \omega} \right]^K \quad (1.19)$$

the superscript (k) is dropped from (1.19) since all A_n 's and a_n 's are identical for the K RVs. Both forms given in (1.18) and (1.19) can be *expanded* to be rewritten as:

$$\tilde{\Phi}_W(\omega) = \sum_{m=1}^M A_m^{(W)} e^{-a_m^{(W)} \omega} \quad (1.20)$$

where the constants $A_m^{(W)}$ and $a_m^{(W)}$ are computed in terms of $A_n^{(k)}$'s and $a_n^{(k)}$'s. It can be noted that $\tilde{\Phi}_{Z_k}(\omega)$ and $\tilde{\Phi}_W(\omega)$ are both written as weighted exponential sum of N and M terms, respectively. M is equal to N^K for the INID case, while it is $\binom{N+K-1}{N-1}$ for the IID case. In [14] it is shown that even for the case of correlated Z_k 's, $\tilde{\Phi}_W(\omega)$ can still be written in a form similar to the one given in (1.20). We refer to the forms in (1.18) and

(1.19) as the *unexpanded* forms, while the form given in (1.20) is referred to as the expanded form.

The approximate PDF for the sum of lognormal RVs W is given by the following equation in [14]:

$$\tilde{f}_W(z) = \frac{1}{\pi} \operatorname{Re} \left\{ \sum_{m=1}^M A_m^{(W)} / (jz + a_m^{(W)}) \right\} \quad (1.21)$$

The expanded form of $\tilde{\Phi}_W(\omega)$ is very useful, since it allows for the evaluation of the approximate CDF to be directly obtained by integrating (1.21) term-by-term and twice to obtain the following equation in [14]:

$$\tilde{F}_W(z) = \operatorname{Re} \left\{ \frac{j}{\pi} \sum_{m=1}^M A_m^{(W)} \ln \left(a_m^{(W)} / (jz + a_m^{(W)}) \right) \right\} \quad (1.22)$$

Unfortunately, for the case of large N and/or large K , the number of terms M for the expanded form is prohibitively large leading to significant rounding errors in the evaluation of (1.20) or subsequently in (1.22).

Various types of approximations have been suggested to approximate the sum of lognormal RVs. In [22], it is mentioned that based on the variances, three types of lognormal RVs sums are identified: narrow ($\sigma^2 \ll 1$); moderately broad ($\sigma^2 < 1$); and very broad ($\sigma^2 \gg 1$). It is shown that the sum of lognormal RVs may be approximated by a Gaussian distribution for the narrow case and as a lognormal distribution for the moderately broad case. For the very broad case, due to the asymptotic character of the

lognormal distribution described in [23], neither Gaussian nor lognormal approximation is appropriate. The next chapter will present a wider review of the famous approximation techniques for the sum of lognormal RVs.

1.2.3 Normal Probability Scale

It is convenient to look at the CDF of the sum of lognormal on a normal probability scale [24], where the lognormal distributions map into straight lines. On this scale, the CDF for a single lognormal RV plotted versus the logarithm of the abscissa generates a straight line plot with a slope that is inversely proportional to the standard deviation parameter, σ . Plotting the CDF for the sum of lognormal RVs on a normal probability scale serves to identify how close or how far the obtained CDF is from that of a pure lognormal RV. Beaulieu in [24] shows that it is convenient to look at the CDF of the sum of lognormal RVs on a normal probability paper.

The initial work in this field mainly assumed that the sum of lognormal RVs may be well approximated by a single lognormal RV. However, based on recent approximations and empirical evaluations in the literature, it is noticed that the sum of lognormal CDF is concaved downward, when plotted on a normal probability scale. Moreover, it is recognized that the CDF of the sum of independent lognormal RVs cannot be reasonably approximated by an equivalent single lognormal RV. The concavity of the CDF of the sum increases as the number of individual lognormal RV components increases. Figure 1.2 plots the CDF of the sum of K lognormal RVs for K equal to 1, 6, 10, and 20. The plot clearly shows that the CDF for the case of $K = 1$, representing a single lognormal RV, is a straight line. As K increases, the resulting CDF deviates

progressively from the straight line shape. The shown results are for sum of IID lognormal RVs of μ_{dB} and σ_{dB} values equal to 0 and 12 dB, respectively.

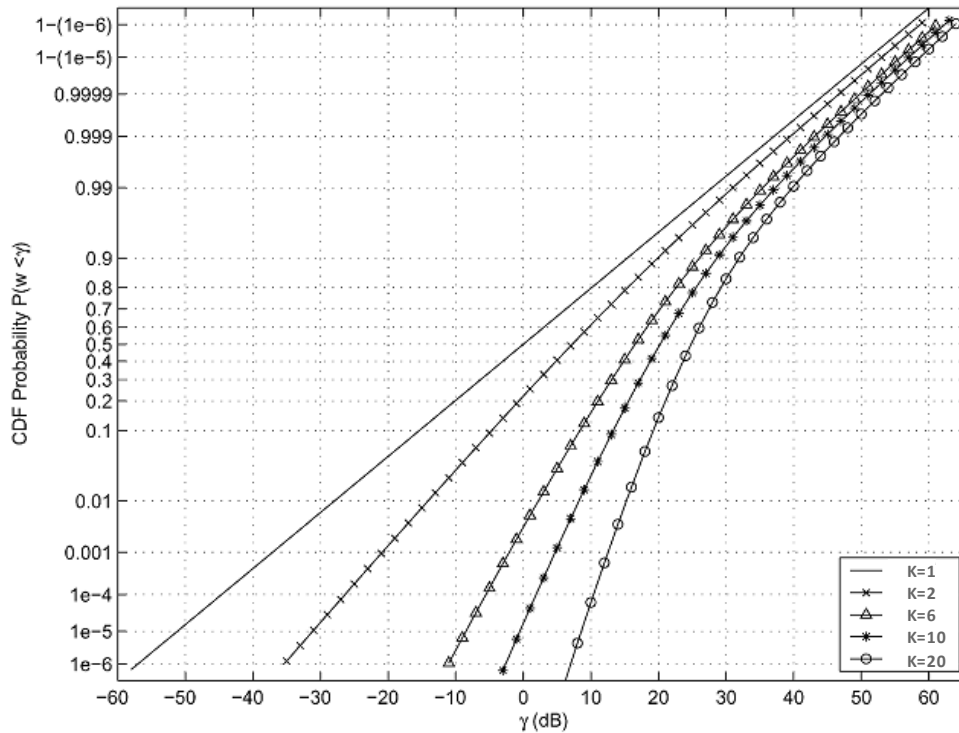


Figure 1.2: CDF of the IID sum of lognormal RVs plotted on a normal probability scale with $\mu=0$ and $\sigma =12$ dB for various values of K [24].

1.3 Problem Statement

The work in this thesis focuses on trying to develop an efficient and convenient evaluation of the distribution of the sum of lognormal RVs $\tilde{F}_W(z)$, by utilizing the *unexpanded* form of the corresponding characteristic function, $\tilde{\Phi}_W(\omega)$, specified by the relations given by (1.18) or (1.19). The new method should avoid utilizing forms similar to, or derived from, the expansion in (1.20) in order to improve the accuracy of the

computations. Furthermore, the proposed work shall focus only on the case of independent and identically distributed lognormal RVs.

In addition, the work in this thesis will attempt to apply the developed method for the DS-CDMA cell-site traffic power characterization problem, which will be described in more detail in Chapter 5.

1.4 Thesis Contributions

The contributions of this thesis work are as follows:

- Implemented efficient methods of computing the distribution function of the sum of lognormal random variables.
- Applied the Epsilon algorithm in approximating the distribution function, which resulted in the number of terms required for approximating the distribution function being significantly reduced when compared to the first implementation.
- Implemented the Legendre-Gauss Quadrature (LGQ) approach of approximating the CF of a lognormal RV, and then use the result to evaluate the CDF of the sum of lognormal RVs.
- Applied the computations of the CDF for the sum of independent LN RVs to a practical resource management problem for DS-CDMA data system.

Chapter 2

LITERATURE REVIEW

This chapter reviews the main existing approximation methods for computing the sum of lognormal random variables in the related literature. Numerous approximate solutions have been developed in literature to compute the moments of the sum of lognormal RVs. In general, it has been shown in [24-26], that every developed approach has its own strength and weakness in terms of the approximation accuracy for solving this problem. Moreover, most of the approximations either provide good accuracy only in some regions (e.g., right and left tails of the distribution) of the sum of the lognormal distribution, but give an unacceptable loss of accuracy in other ranges of the distribution [24]. Others require to judiciously adjust the matching parameters as a function of the PDF region to be approximated [25, 27]. This chapter will describe briefly some of those main approximations.

Loosely speaking, the proposed techniques and approximations in the literature can be classified into different distinct methods, such as, the Moment Matching Approximation (MMA) method which is also known as the Method of Moments (MoMs), e.g. [6, 28], MoMs in the logarithmic domain, e.g. [29], Characteristic Function (CF) method, e.g. [14, 24], upper and lower bounds, e.g. [30-31], and Moment Generating Function Matching (MGFM), e.g. [25-26]. The above methods or techniques are commonly known and mentioned widely in the literature. In this chapter the approximation methods are classified into three distinct groups. The first group relies on

the fact that the distribution of the sum of several LN RVs can still be approximated by the distribution of an equivalent LN RV, whose parameters μ and σ must be computed using the original LN RVs' parameters. Approximation methods belonging to the second group rely on approximating the distribution of the sum of LN RVs by a specific distribution such as log-shifted gamma or Pearson distribution. For methods belonging to group I and group II, the equivalent target approximating distribution, whether a LN or some other distribution, is determined by matching the first few moments, typically two or more, of the sum, to those of the target distribution. The third group of approximation methods develops expressions for the final distribution, which are different from those standard distributions used for group I or group II solutions. Many of the approximation methods must rely on quantities that are either computed empirically, i.e. using Monte-Carlo simulations, or using numerical integrations which limit their versatility.

The approximation methods in the first group represent the earliest work on the subject by Fenton [28] where it is assumed that the sum of lognormal RVs can be approximated by another lognormal RV, by matching its first two positive moments. This procedure is progressively continued until the approximation using a final equivalent LN RV is found. This is one of the earliest methods for solving our problem that is also referred to as the Fenton-Wilkinson method, and which can be also described as a Positive Moment-Matching method. In [29], it is stated that Wilkinson's approach is consistent with an accumulated body of evidence indicating that, for the values of K (number of RVs) of interest, the distribution of the sum of lognormal random variables is well approximated, at least to the first-order, by another lognormal distribution. But this approach is valid only for a limited range of small values of the dB spread σ_{dB} . In

particular, it is reported that the Wilkinson approach breaks down for $\sigma_{\text{dB}} > 4$ dB which includes the range of most practical interest. Schwartz and Yeh [29] follow the same approach as Fenton's, but perform exact computations to match the logarithm of the sum of two independent LN RVs to an equivalent normal RV. The developed method is applicable to a wider range of parameters of the individual LN RVs. It was used in [8, 32], to analyze outage probability in cellular systems. It is further described in [33] as an exact expression for the first two moments of a sum of two lognormal RVs. Employing a recursive approach, the moments are calculated for the sum of more than two lognormal RVs by assuming that a sum of two lognormal RVs is also a lognormal RV.

Later on, Safak in [34] extends the Schwartz and Yeh method to the case of correlated RVs. Mehta *et al.* in [25] propose a method that matches an expression for the characteristic function (CF) of the sum of LN RVs to the CF function of the target equivalent LN RV. Therefore, this method utilizes the frequency domain to perform the matching procedure at two specific frequency points in order to determine the parameters μ and σ for the final equivalent LN RV. The method identifies two sets of two frequency points: the first set produces an equivalent LN RV that approximates the distribution of the sum for high values of the abscissa, while the second set produces an equivalent LN RV that approximates the distribution of the sum for low values of the abscissa.

Approximating the sum of LN RV by an equivalent LN RV produces an approximation that cannot be accurate for all range of the abscissa. For example, the method proposed by Fenton produces an approximation that is suitable for the high end of the distribution (i.e. large values of the abscissa). While the approximation proposed

by Schwartz and Yeh produces an approximation that is suitable for the low end of the distribution (i.e. low values of the abscissa). As mentioned earlier, the method presented by Mehta *et al.* produces an approximation that either fits for the high end or fit the low end of the distribution, but not for both. Realizing this observation, Beaulieu and Xie [24] developed yet another approximation using a LN RV, referred to by the minmax approach, that intends to provide a compromise and attempt to approximate the distribution for the sum in both the high end and also the low end of the abscissa.

Beaulieu and Rajwani in [35] evaluate the empirical CDF for the sum of LN RVs using Monte-Carlo simulations and provide the corresponding plots using the normal probability scale. The CDF of a pure LN RV would appear as a straight line when plotted on the normal probability scale. The obtained results clearly indicate that the distribution for the sum of LN RVs cannot be approximated by single LN RV, especially for sums of large number ($K \geq 6$) of LN RVs as the concavity of the corresponding distribution increases. The study considers the case of sums of IID LN RVs and provides a curve fit for the resulting empirical distribution.

Example methods belonging to the second group include the methods proposed in [22, 36-38]. The study in [22] proposes the use of the log-shifted gamma (LSG) distribution as an approximation for the sum of LN RVs. Similar to the iterative procedure by Fenton [28] and by Schwartz and Yeh [29], the study assumes that the LSG distribution can approximate the sum of the first two LN RVs. Subsequently, the study further assumes that the LSG distribution can also approximate the sum of one LN RV and the obtained LSG distribution from the previous stage. The matching process relies

on the first two moments and involve very cumbersome and hard to evaluate numerical integrals that are required at every stage. In [36] Liu *et al.* suggest that the formulas used for the curve fit in [35] are a special case of a generalized lognormal distribution and propose the use of the power lognormal distribution with finite moments for the approximation for the sum of LN RVs. The empirical CDF for the sum is first evaluated and then employed in the matching process.

Another example of a distribution that has been used to approximate the sum of lognormal RVs in recent work is the Pearson distribution. The Pearson system [39], developed by Pearson in the late 1880s, consists of seven types of distributions covering various distribution functions, among the seven types of Pearson distributions. In [39], Pearson proposed a set of four-parameter PDFs that are referred to as the Pearson's family. The set consists of seven types of fundamental distributions which are tabulated in Table 2.1 [38].

Table 2.1: Seven Types of Pearson Distributions [38]

Model Type	PDF	Distribution Name
I	$f(x) = \frac{1}{B(p,q)} x^{p-1} (1-x)^{q-1}, x \in [0,1]$	Beta Distribution
II	$f(x) = \frac{1}{aB(0.5, m+1)} \left(1 - \frac{x^2}{a^2}\right)^m, x \in [-a, a]$	N/A
III	$f(x) = k \left(1 + \frac{x}{a}\right)^p e^{-px/a}, x \in [-a, \infty]$	Gamma Distribution
IV	$f(x) = v \left(1 + \frac{(x - \mu_4)^2}{\mu_3^2}\right)^{-\mu} \exp\left[-\mu_2 \tan^{-1}\left(\frac{x - \mu_4}{\mu_3}\right)\right], x \in [-\infty, \infty]$	N/A
V	$f(x) = \frac{\gamma^{p-1}}{\Gamma(p-1)} x^{-p} e^{-\gamma/x}$	N/A
VI	$f(x) = \frac{1}{B(b,q)} \frac{x^{p-1}}{(1+x)^{p+q}}, x \in [0, \infty]$	Beta of the Second Kind
VII	$f(x) = \frac{1}{aB(0.5, m-0.5)} \left(1 + \frac{x^2}{a^2}\right)^{-m}, x \in [-a, a]$	Student's t

Zhang and Song in [38] suggest that the distribution for the sum of LN RVs can be approximated by one of the seven types of Pearson distributions. The matching process utilizes the first four moments that need to be evaluated using numerical integration or empirically using Monte-Carlo simulation. In [40], it is found that the Type IV Pearson distribution has the closest PDF and CDF shapes to the lognormal sum distribution. The study proposes to approximate the sum of lognormal distribution with the Type IV Pearson distribution by matching the mean, the variance, the skewness and the kurtosis of the two distributions. The work in [26, 41-42] also uses type IV Pearson distribution for the approximation. The PDF of the Pearson Type IV distribution is defined over the entire real axis and can be written as follows:

$$f_{PIV}(x) = v \left[1 + \frac{(x + \mu_4)^2}{\mu_3^2} \right]^{-\mu_1} \exp \left[-\mu_2 \tan^{-1} \left(\frac{x - \mu_4}{\mu_3} \right) \right] \quad (2.2)$$

Wu *et al.* in [37] propose the use of log-skewed normal distribution as an approximate distribution for the sum of LN RVs. Again all the above methods require either the utilization of empirical results obtained from Monte-Carlo simulations or evaluating nested numerical integrations.

Finally, for methods belonging to the third group, the work by Beaulieu and Rajwani in [35] referenced earlier proposes the form $\Psi(a_0 - a_1 e^{a_2 z})$ where $\Psi(\cdot)$ is the CDF of the standard normal random variable, and a_0 , a_1 , and a_2 are constants determined by matching the form of the distribution to the empirical distribution in the desired range of the abscissa z . The study in [43] by Zhao and Ding proposes a least-squares approximation of the form $\Psi(a_0 + a_1 z)$ for the sum of LN RVs approximation, or the form $\Psi(a_0 + a_1 z + a_2 z^2)$ for the quadratic least squares approximation. Again, the required constants are determined such that the error between the forms and the empirical CDF for the sum is minimum. Finally, the recent work by Mahmoud in [14] develops expressions for the characteristic function for the sum variable for both the independent and correlated cases. The expressions are in the form of weighted exponential sums which allow for a double integration to obtain a summation expression for the target approximate CDF. The evaluations performed in [14] reveal that the developed expressions are simple and convenient to evaluate for a sum of a low number (i.e. ≤ 6) of LN RVs, while the difficulty increases with both the increase in the number of individual LN RVs and also with the increase in the number of corresponding σ 's.

Chapter 3

METHODS OF ENHANCING THE COMPUTATIONS OF THE DISTRIBUTION FUNCTION OF LN RVs

In this chapter, efficient and convenient computation methods for the sum of a large number of LN RVs will be presented, by utilizing the *unexpanded* form for the characteristic function of the sum of lognormal RVs as in equation (1.19). The first method is the application of appropriate quadrature rules to the integral involving the characteristic function for the sum with a proper change of variables. The second method is the application of the Epsilon algorithm to reduce the number of needed computations. Results indicate that while the first method presents a simple way to evaluate the sum in terms of the weights and nodes of the chosen quadrature rule, it is computationally heavy as it may require 100s to 1000s of terms to arrive at a reasonable approximation of the target CDF. The second method reduces the needed evaluations to as few as 10 and improves the accuracy for both the lower end and higher end of the approximated CDF.

3.1 Use of Oscillatory Quadratures

In this section, different quadrature rules are listed and briefly presented. Many quadrature types are reviewed in the literature, such as: Fejer [44], Clenshaw–Curtis [45], or Gauss quadratures family, that include different types depending on the weight function. More details on this can be found in [21]. The highly oscillatory quadrature is

discussed in [46-47]. In [48] a comparison is made between Clenshaw–Curtis and Gauss quadrature, while the work in [49] compares between Fejer and Clenshaw–Curtis quadratures. The work in [50-51] focuses mainly on the error estimation for these quadratures. More related material can be found in [52-53].

Quadrature rules are in general used to approximate a definite integral of a function, which is, stated as a weighted sum of function values at specified points within the domain of integration. The N -point Gaussian quadrature rule is a quadrature rule constructed to yield an exact result for polynomials of degree $2N - 1$ or less by a suitable choice of the points x_i and weights w_i for $i = 1, \dots, N$. The domain of integration for quadrature rules is conventionally taken to be $[-1, 1]$, and the rule can be stated as follows:

$$\int_{-1}^1 f(x) dx \approx \sum_{i=1}^N w_i f(x_i) \quad (3.1)$$

The above Gaussian quadrature produces accurate results if the function $f(x)$ is well approximated by a polynomial function in the interval $[-1, 1]$. The integrated function can be written as $f(x) = W(x)g(x)$, where $g(x)$ is approximately polynomial, and if $W(x)$ is known, then there are alternative weights w'_i such that $\int_{-1}^1 f(x) dx = \int_{-1}^1 W(x)g(x) dx \approx \sum_{i=1}^N w'_i f(x_i)$. Common weights functions include $W(x) = (1 - x^2)^{-\frac{1}{2}}$ for the Chebyshev–Gauss quadrature, and $W(x) = e^{-x^2}$ as in the Hermite–Gauss quadrature (HGQ) [21]. When the integral is over the interval $[a, b]$, then the limits are changed into $[-1, 1]$ as the follows:

$$\int_a^b f(x)dx = \frac{b-a}{2} \int_{-1}^1 f\left(\frac{b-a}{2}x + \frac{b+a}{2}\right) dx \quad (3.2)$$

using the Gaussian quadrature rule, the integral in (3.2) may be approximated as:

$$\int_a^b f(x)dx \approx \frac{b-a}{2} \sum_{i=1}^n w_i f\left(\frac{b-a}{2}x_i + \frac{b+a}{2}\right) \quad (3.3)$$

3.2 Using Quadratures to approximate CDF of sum of LN RVs

The *unexpanded* form for $\tilde{\Phi}_W(\omega)$ in equation (1.18) or (1.19) is relatively accurate especially for large K (i.e. $K > 40$, number of RVs). The approximate CDF $\tilde{F}_W(z)$ may be evaluated from the approximate CF using [19]:

$$\tilde{F}_W(z) = \frac{2}{\pi} \int_0^{\infty} \frac{\text{Re}\{\tilde{\Phi}_W(\omega)\}}{\omega} \sin(\omega z) d\omega \quad (3.4)$$

The previous relation is reasonably accurate for small and moderate values of the abscissa z . For large z , the oscillations of the term $\sin(\omega z)$ become very excessive. This is compounded by the fact that the envelope dominated by $\tilde{\Phi}_W(\omega)$ does not decay sufficiently fast especially for large σ_k 's (i.e. $\sigma_k > 3$). An easier form of (3.4) can be obtained by performing the substitution $y = \omega z$. Then the new approximation for the CDF for the sum RV W is now given by the following relation:

$$\tilde{F}_W(z) = \frac{2}{\pi} \int_0^{\infty} \frac{\text{Re}\{\tilde{\Phi}_W(y/z)\}}{y} \sin(y) dy \quad (3.5)$$

The above form eliminates the oscillations due to the sine function. However, due to the argument y/z for the CF of W , the envelope need to be considered for excessively large values of the argument of $\tilde{\Phi}_W(\cdot)$ when z is small.

This thesis work attempts to utilize the relatively accurate CF of the sum of IID lognormal RVs specified by (1.19) in the computation of the approximate CDF of the same sum. Towards this end, the work utilizes different quadrature rule to evaluate the approximate CDF using relation (3.5)

For a given quadrature rule with N_q number of points, β_n weights, and nodes α_n , the approximate CDF in (3.5) can be evaluated using (3.3) as:

$$\tilde{F}_W(z) \approx \sum_{n=1}^{N_q} \beta_n g(\alpha_n) \quad (3.6)$$

where the function $g(\cdot)$ is given by

$$g(\alpha_n) = \frac{2}{\pi} \operatorname{Re}\{\tilde{\Phi}_W(\alpha_n/z)\} \sin(\alpha_n)/\alpha_n \quad (3.7)$$

The relation in (3.6) provides an expression for evaluating the approximate CDF for the sum W in terms of the original parameters μ_k 's and σ_k 's of the Z_k 's RVs and the HGQ weights and nodes as well as the weights β_n , and nodes α_n used in (3.6). In the subsequent section, equation (3.6) is evaluated using three quadrature rules: namely Clenshaw-Curtis (CC), Fejer2, and Legendre. It should be pointed out that the first two quadratures are preferred for oscillatory integrands [49].

3.3 Application of the Epsilon Algorithm

The development from the previous section indicates that while the sum W of K LN RVs can now be evaluated using a simple summation expression in terms of the primitive parameters and quadrature constants. It still requires the evaluation of a large number (from several hundreds to several thousands) of terms, depending on K , σ_k 's, and the quadrature rule employed. In this subsection the Epsilon algorithm of [54] and [55] is employed to facilitate evaluating (3.5) with fewer computations.

Towards the end of this subsection, it is noted that the integral in (3.5) can be written as a sum of integrals, each being evaluated over a period of the oscillating sine term. Specially, it can be written as the following equation [15]:

$$\begin{aligned}\tilde{F}_W(z) &= \frac{2}{\pi} \sum_{l=0}^{\infty} (-1)^l \int_0^{\pi} \frac{\operatorname{Re}\{\tilde{\Phi}_W((l\pi + t)/z)\}}{(l\pi + t)} \sin(t) dt \\ &= \frac{2}{\pi} \sum_{l=0}^{\infty} (-1)^l x_l\end{aligned}\tag{3.8}$$

where x_l^{th} term is equal to the $\int_0^{\pi} \frac{\operatorname{Re}\{\tilde{\Phi}_W((l\pi+t)/z)\}}{(l\pi+t)} \sin(t) dt$. For the evaluation of (3.8), typically the first L terms, for some large L , are evaluated only. Then, the approximate CDF is given by the following equation:

$$\tilde{F}_W(z) \approx S_L = \frac{2}{\pi} \sum_{l=0}^L (-1)^l x_l\tag{3.9}$$

To obtain a good approximation for $\tilde{F}_W(z)$, and due to the nature of $\tilde{\Phi}_W(\omega)$, the specified summation in (3.9) converges only for extreme values of L , especially for large z . The

intention is to reduce the number of computations required to arrive at $\tilde{F}_W(z) = \lim_{L \rightarrow \infty} S_L$. This is achieved through the utilization of the Epsilon algorithm.

The Epsilon algorithm of [54] and [55] operates as follows: Build a table similar to that shown in Table 3.1. The table, referred to by the ϵ -table, has columns for $r = -1, 0, 1, 2, \dots$ and rows for $l = 0, 1, 2, \dots$. The $r = -1$ column is initialized to contain zeros, while the $r = 0$ column is initialized to contain the partial sum S_l in the l^{th} row. For the remaining entries in the ϵ -table, the entry in the l^{th} row and r^{th} column is given as:

$$\epsilon_{r+1}^{(l)} = \epsilon_{r-1}^{(l+1)} + \left[\epsilon_r^{(l+1)} - \epsilon_r^{(l)} \right]^{-1} \quad \text{for } r = 0, 1, 2, \dots \quad (3.10)$$

The even columns of the ϵ -table now contain increasingly more accurate estimates of S_∞ or $\tilde{F}_W(z)$. In the results section it is shown that for as few as 5 or 10 terms, using the Epsilon algorithm one can obtain a reasonable approximation for $\tilde{F}_W(z)$ in the range of interest. Finally, it should be noted that Tellambura and Senaratne in [15] utilize the Epsilon algorithm to compute the CDF for W , $\tilde{F}_W(z)$, where the corresponding integration involves numerical integrations to evaluate $\tilde{\Phi}_{z_k}(\omega)$ and then $\tilde{\Phi}_W(\omega)$. In addition, the evaluations in [15] are chosen for moderate values of σ_k to allow more accurate evaluation of $\tilde{\Phi}_W(\omega)$.

Table 3.1: The Epsilon algorithm table

		r					
l	-1	0	1	2	3	4	...
0	0	S_0	ϵ_1^0	ϵ_2^0			
1	0	S_1	ϵ_1^1	ϵ_2^1	ϵ_3^1		
2	0	S_2	ϵ_1^2	ϵ_2^2	ϵ_3^2	ϵ_4^2	
3	0	S_3	ϵ_1^3	ϵ_2^3	ϵ_3^3	ϵ_4^3	
4	0	S_4	ϵ_1^4	ϵ_2^4	ϵ_3^4		
5	0	S_5	ϵ_1^5	ϵ_2^5	ϵ_3^5		
...							

Progressively more accurate estimates of S_∞ for even values of r .

3.4 Numerical Results and Discussion

For the evaluation results of the CDF, curves are plotted on a normal probability scale with the abscissa z in dBs. Similar to most of the work in the literature, the range of probabilities on the y -axis is limited to be from 10^{-6} to $(1 - 10^{-6})$. The normal probability scale serves to reveal the matching between the original CDF and the approximation for both low and high ends of the distribution.

First, the form (3.6) is evaluated for the three considered quadratures: Clenshaw-Curtis (CC), Fejer2, and Legendre. The approximation resulting from (3.6) for different numbers of nodes and weights is shown in Figure 3.1 for $K = 20$ and for σ_{dB} equal to 6 dB and 12 dB.

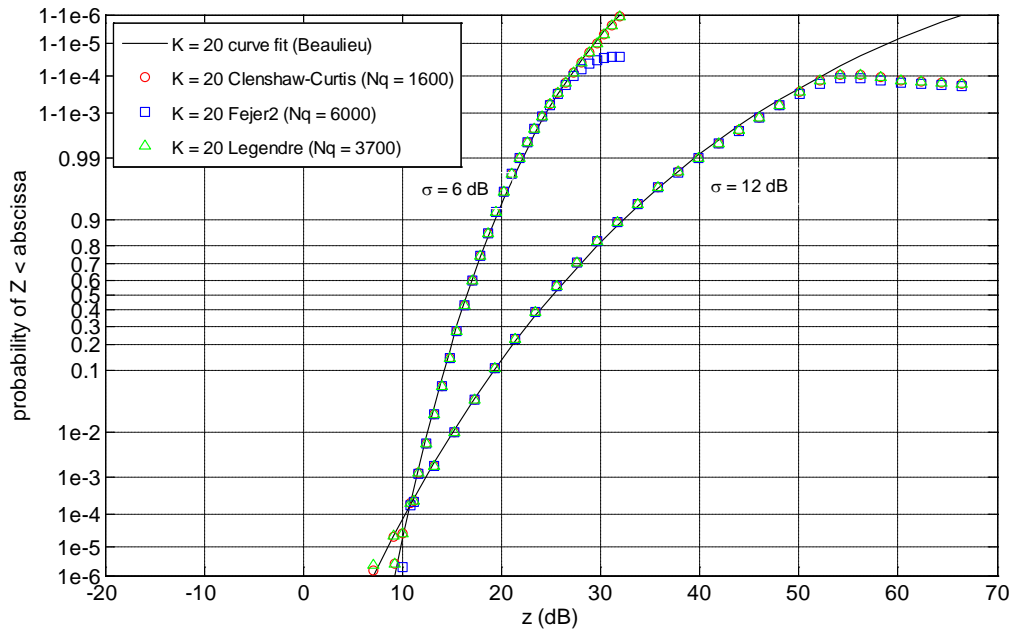


Figure 3.1 The CDF of the sum of $K=20$ IID lognormal RVs $\mu_{\text{dB}}=0\text{dB}$ and $\sigma_{\text{dB}}=6\text{dB}$ and $\sigma_{\text{dB}}=12\text{dB}$ using the curve fit in [35] and three quadrature rules: Clenshaw-Curtis, Fejer2, and Legendre.

The approximated CDF is plotted against the original CDF as represented by the curve fit developed in [35]. The number of weights and nodes N_q , considered for this evaluation is 1600, 6000, and 3700 for the CC, Fejer2, and Legendre quadrature rules, respectively. CC and Fejer2 quadrature rules are specialized for oscillatory integrands, while the Legendre quadrature rule is for general integrands. The CC quadrature rule produces the best results with the least N_q . It can be seen that for the same quadrature rules, the evaluation is less accurate for $\sigma_{\text{dB}} = 12\text{dB}$ compared to those for $\sigma_{\text{dB}} = 6\text{dB}$. This is because $\Phi_W(\omega)$ decays more rapidly for small values of σ_{dB} than it does for high values of σ_{dB} such as 12 dB. Another observation is that the quadrature rules seem to be able to approximate the desired CDF for low and moderate values of the abscissa, but the discrepancies arise mostly for higher values of the abscissa. To assess the relative

accuracy between the approximate CDF and the original CDF, the following metric is developed: define the set of I abscissa points z_i uniformly spaced between $10 \log_{10} z_{\min}$ and $10 \log_{10} z_{\max}$ in the range of interest. The sum of relative errors squared, $SSRE$ is defined as

$$SSRE = \sum_{i=1}^I \left[\frac{\Psi^{-1}(F_W(z_i)) - \Psi^{-1}(\tilde{F}_W(z_i))}{\Psi^{-1}(F_W(z_i))} \right]^2 \quad (3.11)$$

where $F_W(z_i)$ is the true CDF for the sum W evaluated at z_i , $\tilde{F}_W(z_i)$ is the approximate CDF evaluated at z_i , and $\Psi^{-1}(\cdot)$ is the inverse normal RV CDF. $F_W(z_i)$ is taken as the curve fit developed in [35]. Figure 3.2 shows the $SSRE$ for the three considered quadrature rules versus the number of weights and nodes, N_q , considered in the evaluation of (3.5). The CC quadrature produces the least $SSRE$ for N_q values ranging from few 10s of terms to about 200 compared to the other quadrature rules. For extremely large N_q (i.e. greater than 500), all quadrature rules produce the same $SSRE$ value. The $SSRE$ floor of 2.2×10^{-2} is due to the inaccuracies of the $\tilde{\Phi}_W(\omega)$ approximation, and not due to the quadrature rule. Therefore, increasing the number of weights and nodes N_q does not aid in obtaining more accurate results for $\tilde{F}_W(z_i)$.

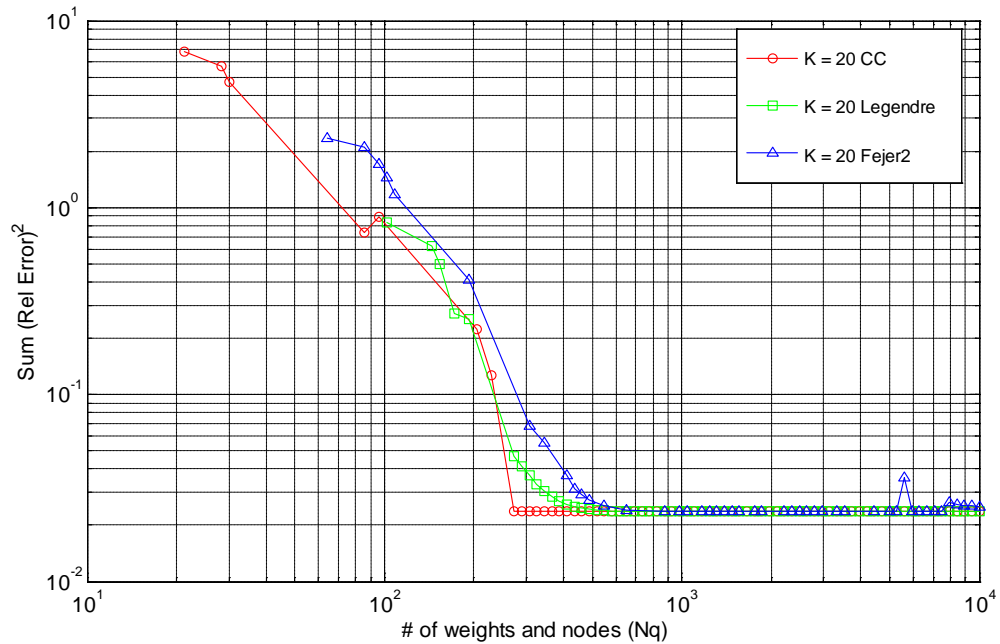


Figure 3.2 Sum of squared relative errors between CDF evaluated using quadrature rules and curve fit versus number of weights and nodes for sum of 20 IID LN RVs and $\sigma_{\text{dB}} = 12$ dB.

Next, the form (3.9) is considered to assess the number of terms L required to obtain a reasonable approximation $\tilde{F}_W(z)$. Figure 3.3 shows the evaluation of (3.9) for $K=20$ and for σ_{dB} equal to 6 dB and 12 dB. The number of terms considered in the partial summation, L is taken to be 200, 1000, and 10000. The individual x_l term is evaluated using the MATLAB `quadgk` [56] numerical integration routine.

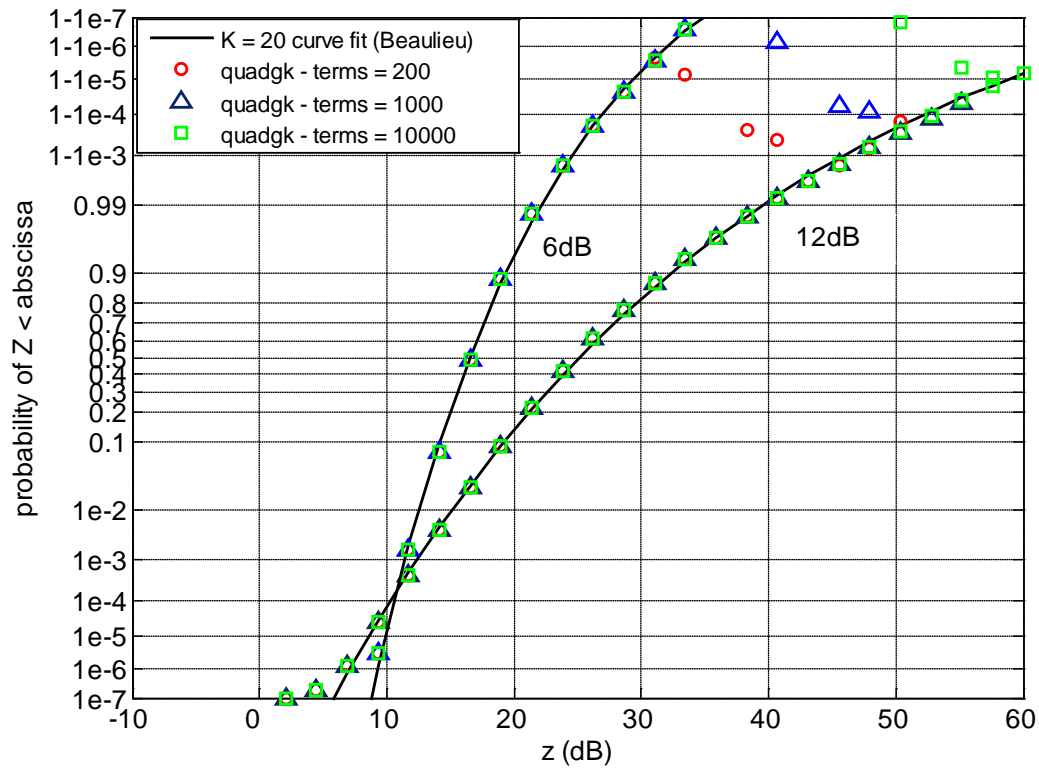


Figure 3.3 The CDF for the sum W evaluated using relation (3.10) for 20 IID LN RVs and σ_{dB} equal to 6 dB and 12 dB.

It can be seen that the accuracy of the approximation improves as L increases. However, to obtain a reasonable close fit for the original CDF, the number of terms L must be on the order of 10^4 or higher. Furthermore, the approximation is less accurate for higher values of the abscissa z especially for $\sigma_{\text{dB}} = 6$ dB. In Figure 3.4, the results are shown for evaluating (3.9) but using the Epsilon algorithm for K equal to 6 and 20 and $\sigma_{\text{dB}} = 12$ dB. For this evaluation 6, 10, or 14 terms are utilized of x_l to construct the Epsilon table. It can be seen that with as few as 6 terms and with the use of the Epsilon algorithm, one can obtain an approximation that is better than that obtained with 1000's of terms using other than the Epsilon algorithm. Furthermore, the accuracy of the approximation for the low end and high end of the distribution improves compared to the

results in Figure 3.3. Finally, more accurate results are possible with a higher number of initial terms of x_l .

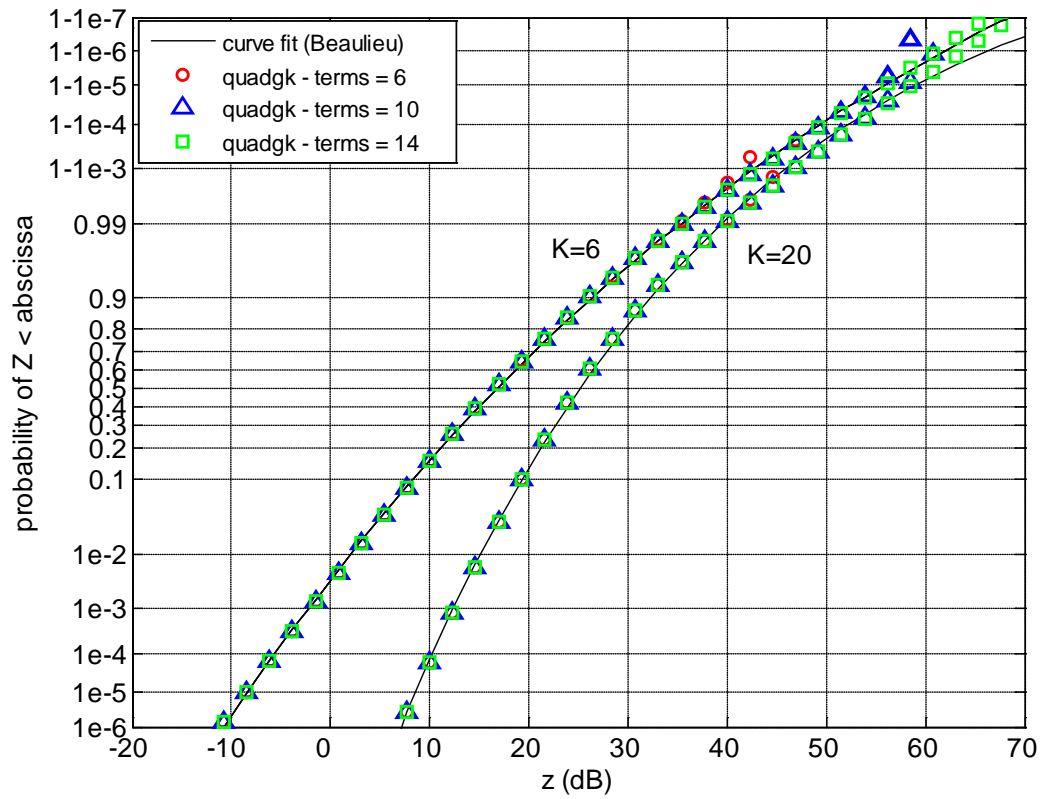


Figure 3.4 The CDF for the sum W evaluated using the Epsilon algorithm for 6 and 20 IID LN RVs and σ_{dB} equal 12 dB.

Chapter 4

ANALYSIS AND IMPLEMENTATION OF LEGENDRE-GAUSS QUADRATURE

The previous work in chapter 3 utilizes the CF for the single RV specified by relation (1.17) developed in [20] and [14] to compute the CDF for the sum of lognormal RVs. Initially, the CF for the sum of independent K lognormal RVs is simply the multiplication of the individual CFs, and then the CDF may be approximated using the relation (1.22) for moderate values of M or using the general relation (1.16). Chapter 3 focused on exploiting (1.16) since the focus is on cases where M is extremely large since K and/or N are large.

The CF utilized in the approach described above uses the HGQ rule to approximate the original integral with infinite limits of the CF specified by relation (1.11). Gubner in [20] has shown an example explaining that using the Legendre-Gauss Quadrature rule (LGQ) as opposed to the HGQ one can obtain higher accuracy for the same number of nodes and weights if the infinite limits of the integral are changed to optimized finite integral limits. The example evaluated the CF for a single RV at one frequency point to highlight the relative accuracy of the involved quadrature rules.

The work in this chapter extends the work of Gubner in [20] and evaluates the CF of the single RV with assessment of the accuracy of the LGQ relative to the HGQ used by Mahmoud in [14] for the entire frequency range of interest. In addition, the work tries to

obtain a new expression for the CF of the single RV based on the LGQ rule that may be of acceptable accuracy but with a lower number of terms N , as compared to the HGQ rule.

4.1 Evaluation of the CF of LN RV Using Optimized Integral Limits

The CF for the LN RV Z with parameters μ and σ may be computed using the integral in relation (1.11). Gubner in [20] produces an alternative integral for the case of a lognormal RV with reduced oscillation specified by

$$\tilde{\Phi}_Z(\omega) = c \int_{-\infty}^{\infty} e^{-\omega e^t} e^{-j\pi t/(2\sigma^2)} e^{-(t/\sigma)^2} dt \quad (4.1)$$

where the constant c is equal to $e^{[(\pi/(2\sigma^2))/2]}/(\sqrt{2\pi}\sigma)$. Noticing the infinite integral limits in (4.1) and taking the term $e^{-(t/\sigma)^2}$ as the weight function, immediately points to the HGQ rule as the appropriate or natural approximation method. Gubner also observed that the envelope of the integrand in (4.1) attains its maximum at $t_0 < 0$ which is the solution of $e^t = -t/(\omega\sigma^2)$. Furthermore, t_0 goes to minus infinity as the product $\omega\sigma^2$ goes to infinity. Therefore one may obtain a better approximation of (4.1) if only the significant part of the integrand is considered by performing the integral in (4.1) over a finite interval $[a, b]$. The new limits $a < t_0 < b$, referred to herein by the optimized integral limits, are chosen such the envelope at a and b is below a certain threshold relative to the envelope value at t_0 . For the specific frequency point of $\omega = 10^4$ radians/sec and using a threshold of 10^{-16} , Gubner showed that $\tilde{\Phi}_Z(\omega)$ evaluated using

the 45-point LGQ is accurate to the 14th decimal place while that for the 45-point HGQ is only accurate to the 6th decimal place.

4.1.1 Implementation of LGQ with Optimized Integral Limits

In this subsection, we adopt the method developed by Gubner and evaluate the CF of a single LN RV using the LGQ rule with the use of optimized integral limits. For a given ω and a specified threshold, T , the CF specified by (4.1) may be approximated by

$$\tilde{\Phi}_Z(\omega) = c \int_a^b f(t) dt \quad (4.2)$$

where $f(t) = e^{-\omega e^t} e^{-j\pi t/(2\sigma^2)} e^{-(t/\sigma)^2}$ and the limits a and b are chosen such that $f(a) = Tf(t_0)$ and $f(b) = Tf(t_0)$. t_0 is the abscissa point that maximizes $f(t)$. Mapping the integral limits to the interval $[-1, 1]$ and using the relation (3.3), the CF approximation $\tilde{\Phi}_Z(\omega)$ may be evaluated using

$$\tilde{\Phi}_Z(\omega) \approx c \left(\frac{b-a}{2} \right) \sum_{n=1}^N w_n f \left(\frac{b-a}{2} t_n + \frac{b+a}{2} \right) \quad (4.3)$$

where t_n and w_n are the n^{th} node and weight of the N -point LGQ rule. Writing (4.3) in a manner similar to (1.17), we have

$$\tilde{\Phi}_Z(\omega) \approx \sum_{n=1}^N A_n e^{-\omega a_n} \quad (4.4)$$

where now the coefficients a_n and A_n are computed by e^{α_i} and $c\left(\frac{b-a}{2}\right)w_n f(\alpha_i)$, respectively, and α_i is $\left(\frac{b-a}{2}t_n + \frac{b+a}{2}\right)$.

While the form of (4.4) is similar to that of (1.17), unfortunately there is a critical difference between these two forms. The coefficients a_n and A_n in (1.17) are identical for every frequency ω whereas their coefficients in (4.4) are a function of ω because of their dependency on the optimized integral limits. This prevents the utilization of (4.4) in obtaining simple expressions for the PDF or CDF of the sum of lognormal RVs as in (1.21) and (1.22), respectively. Nonetheless, (4.4) still presents a more accurate evaluation of the CF of the single LN RV compared to that of (1.17). The subsection 4.2 will explore alleviating this shortcoming at the cost of sacrificing the accuracy of the approximation.

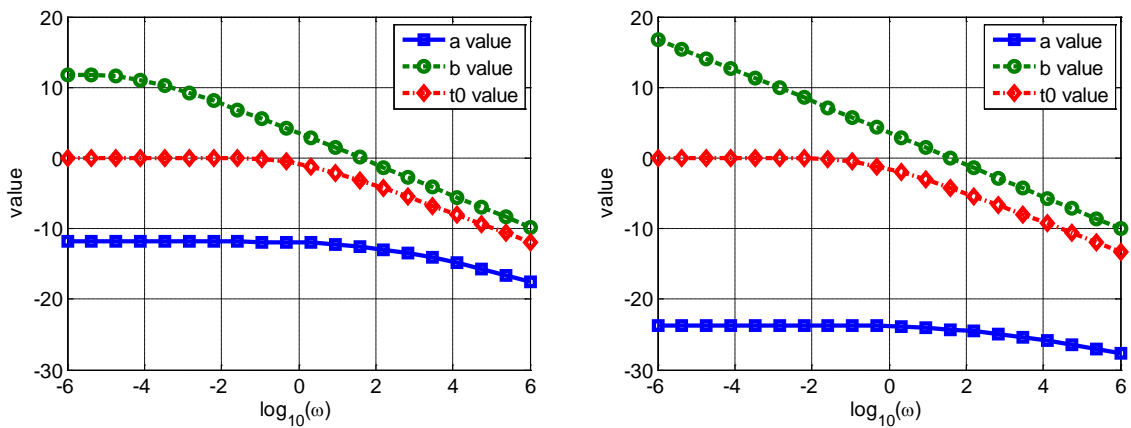
4.1.2 Results and Discussion

In this subsection, we evaluate the accuracy of the new expression for the characteristic function stated by (4.4) relative to the expression obtained by Mahmoud in [14] and reiterated in relation (1.17). Specifically, we will use the relative error defined as

$$\text{Relative Error} = \frac{\left| |\tilde{\Phi}_Z(\omega)| - |\tilde{\Phi}_Z^{\text{REF}}(\omega)| \right|}{|\tilde{\Phi}_Z^{\text{REF}}(\omega)|} \quad (4.5)$$

where $|x|$ is the absolute value of x . $\tilde{\Phi}_Z(\omega)$ is the CF of interest evaluated using (4.4) or (1.17). $\tilde{\Phi}_Z^{\text{REF}}(\omega)$ is the reference (or accurate) value for the CF at the specific frequency of ω radians per second. As stated in the introduction part of this section, the use of 45-point

LGQ with optimized integral limits produces a value of $\tilde{\Phi}_z(\omega)$ that is accurate to the 14th decimal place for $\omega = 10^4$ radians per second. We also evaluate the original integral in (4.1) using Matlab's function `quadgk()` which utilizes the adaptive Gauss-Kronrod quadrature [56] and it is found to be as accurate as the example given above for the LGQ rule. In the rest of the coming material, we consider the numerical evaluation of (4.1) using Matlab's `quadgk()` function to be the accurate value. The evaluation shows that Matlab's `quadgk()` function and the 45-point LGQ with optimized integral limits produce values of $\tilde{\Phi}_z(\omega)$ that are within $10^{-15} \sim 10^{-10}$ of each other and have much higher accuracy relative to all other schemes considered.



a) $\sigma = 1.3816$ ($\sigma_{\text{dB}} = 6$ dB)

b) $\sigma = 2.7631$ ($\sigma_{\text{dB}} = 12$ dB)

Figure 4.1: Evaluation of optimized integral limits for the cases of (a) $\sigma_{\text{dB}} = 6$ dB, and (b) $\sigma_{\text{dB}} = 12$ dB.

Initially, we evaluate the optimized integral limits for (4.1) needed to write the integral in (4.2) with finite limits. The optimized integral limits are evaluated for the case of $\sigma = 1.3816$ (i.e. $\sigma_{\text{dB}} = 6$ dB) or $\sigma = 2.7631$ (i.e. $\sigma_{\text{dB}} = 12$ dB). The optimized

integral limits are shown in Figure 4.1 for the two cases. The curves also depict the corresponding value of t_0 where the envelope of (4.2) attains its maximum. The evaluation is performed for a wide range of the frequency parameter ω . One can note that the envelope attains its maximum at values very close to $\omega = 0$ from the left for frequencies less than 1 radian per second. As ω increases beyond 1 radian per second, the peak shifts towards the negative part of the frequency axis. The figure shows the limits for the case of small standard deviation σ represented by $\sigma_{\text{dB}} = 6$ dB and for the case of large standard deviation represented by $\sigma_{\text{dB}} = 12$ dB. However, for further evaluation of the CF and the evaluation of the relative computational needed effort, we will focus on the case of $\sigma_{\text{dB}} = 12$ dB or large standard deviation. The latter case represents the difficult computation case as the CF decays very slowly with ω and need to be accurate for a very wide range of the frequency parameter.

The relative error is evaluated using (4.5) for the CF computed based on (1.17) and the HGQ rule and also for the CF computed using (4.4) employing the LGQ rule. The evaluation is performed for a different number of quadrature points, namely N equal to 10, 25, and 45. The results are shown in Figure 4.2 for a frequency range extending from $\omega = 10^{-6}$ to $\omega = 10^7$ radians per second. One observation is that for the same number of quadrature points N , the evaluation using the LGQ rule is more accurate compared to that using the HGQ rule. The difference in the relative error value increases with the increase in N with maximum disparity between the two rules for $N = 45$ points. It can be seen that for the LGQ rule with $N = 45$ the relative error is very small compared to the other cases where it ranges from $\sim 10^{-15}$ for very small ω to $\sim 10^{-10}$ for very large ω .

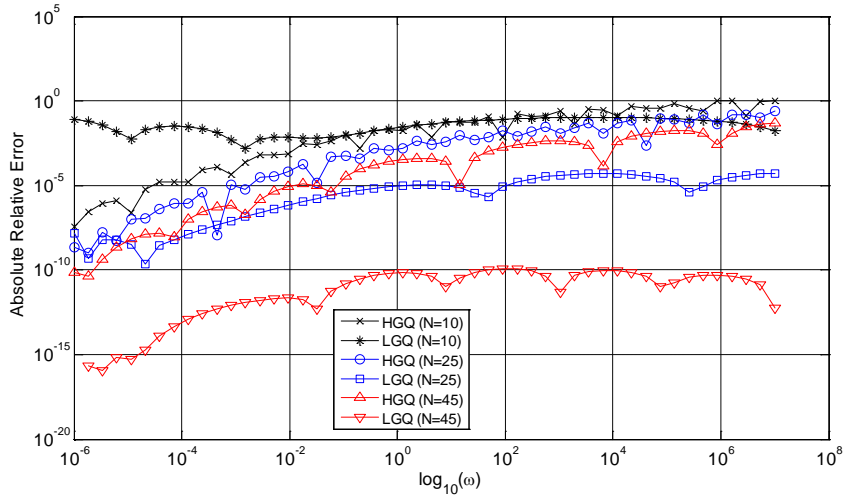


Figure 4.2: Evaluation of relative error for the computation of absolute of CF for $\sigma_{\text{dB}} = 12$ dB using HGQ and LGQ with optimized integral limits.

4.2 Evaluation of the CF of LN RV Using Fixed Integral Limits

To be able to invert the expression in (4.4) for the CF of the single LN RV or the one corresponding to the sum of independent LN RVs resulting from the product of expressions similar to (4.4), the coefficients a_n and A_n have to be independent of the frequency variable ω . In the previous subsection, it was shown that the coefficients a_n and A_n are a function of ω because the integral limits a and b are optimized at every frequency point. In this subsection we will evaluate the accuracy of the new expression for the CF using the LGQ rule but for fixed integral limits.

4.2.1 Implementation of LGQ with Fixed Integral Limits

Let there be fixed integral limits for (4.2), denoted by a^* and b^* , that are not function of the frequency variable ω . Since a^* and b^* represent the lower and upper integration limits, then for a given σ_{dB} and independently of ω the natural choice of a^*

would be the minimum of all possible a values while the choice for b^* would be the maximum of all possible b values. For the data shown in Figure 4.3 and for $\sigma_{\text{dB}} = 12$ dB and $\omega \in (10^{-6}, 10^7)$, the values for a^* and b^* values are equal to -28.827 and 16.733 , respectively. Using these values in the coefficient of (4.4) by replacing the parameters a and b with a^* and b^* , respectively, results in an expression for the CF $\tilde{\Phi}_Z(\omega)$ constant coefficients a_n and A_n that do not depend on ω . The expression in (4.4) based on a^* and b^* can now be utilized in a manner similar to the development in [14] to obtain the CF for the sum of independent LN RVs as in (1.20) and then obtain the PDF of the sum by inverting (1.20) to obtain (1.21). However, in this subsection we are interested in evaluating the accuracy of the new expression with the usage of a^* and b^* .

4.2.2 Results and Discussion

Using the same frequency range and number of quadrature points N as in subsection 4.1.2, we use (4.5) to evaluate the relative error to assess the accuracy of the expression (4.4) using the LGQ rule with fixed integral limits a^* and b^* . Figure 4.3 shows the resulting curves. Similar to Figure 4.2, the figure also includes the evaluation of the relative error for (1.17) which utilizes the HGQ rule for comparison purposes.

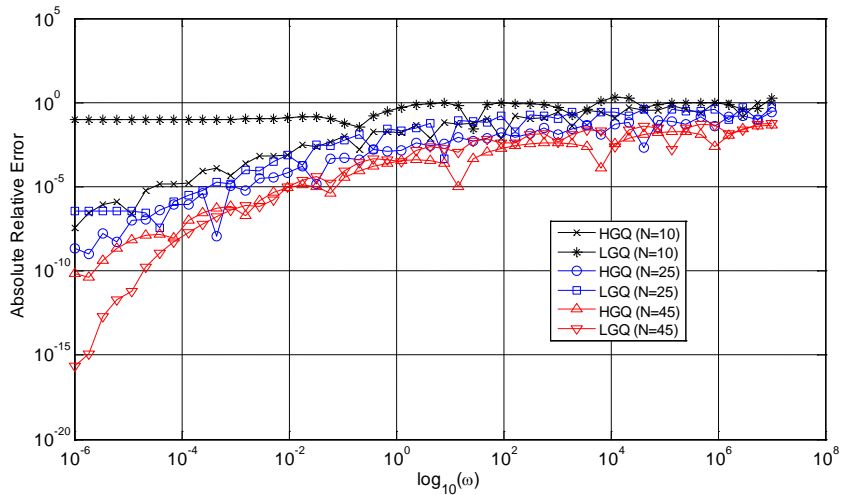


Figure 4.3: Evaluation of relative error for the computation of absolute of CF for $\sigma_{\text{dB}} = 12$ dB using HGQ and LGQ with fixed integral limits a^* and b^* .

It can be seen from Figure 4.3 that the LGQ rule is no longer always more accurate than its HGQ counterpart, for the same number of quadrature points, N . In fact, the LGQ rule is more accurate than the corresponding HGQ rule only for N equal to 45 and only for very low values of the frequency variable ω . For values of ω greater than 10^{-4} radians per second, the LGQ rule performs worse than the HGQ for N equals to 10 and 25. In short, there is no clear advantage of using the LGQ rule for fixed integral limits a^* and b^* . This may be interpreted as follows. Using the extended range of abscissa $[a^*, b^*]$, the nodes N -point LGQ are not distributed in the range where the integrand is most significant, as it is the case for optimized integral limits, but rather are spread over areas of the abscissa that are not significant. This results in a lower accuracy when compared to the optimized case.

Furthermore, the previous two relative error curves were evaluated using the absolute value of the approximate CF. This work also evaluated the relative error in the

computation for the real part and the imaginary part of the CF. It is observed that the relative error in the computation of the imaginary part is very high compared to that for the computation of the real part. In other words, for most of the cases, the relative error in the absolute value of the CF is mainly due to the errors in computing the imaginary part.

Finally, through experimentation it is observed that selecting values other than a^* and b^* defined in this subsection may produce lower relative error curves compared to those shown in Figure 4.3, specifically for particular ranges of the frequency variable ω . Therefore, in this development we seek to identify, in a methodological manner, new and *fixed* integral limits that minimize the relative error for the CF computed using the LGQ rule over the entire range of the frequency variable as a whole. We refer herein to these new integral limits as the quasi-optimized integral limits.

Let a set of frequency points ω_i 's, denoted by Ω be defined such that $\log_{10} \omega_i \in \{-6, -5, \dots, 7\}$. Realizing that the true value of $|\Phi_Z(\omega)|$ decreases rapidly with the increase of the frequency variable and that it is of interest to obtain an approximation that is most accurate where $|\Phi_Z(\omega)|$ is significant, we define a set of weights W_i 's that emphasize the relative error for small ω_i and marginalizes as ω_i increases. For a given pair of integral limits (a, b) , the weighted sum of relative errors (WSRE) is evaluated at the specified frequency points in Ω . The desired fixed quasi-optimized integral limits, denoted by (\hat{a}, \hat{b}) may be obtained by minimizing the sum of weighted relative errors over all possible pairs (a, b) . We restrict the search space to integer values of a and b only where $a < b$. For $\sigma_{\text{dB}} = 12$ dB, the focus of this subsection, and using Figure 4.1, a

and b each range from -30 to 17. For other values of σ_{dB} , the corresponding range for a and b must be used.

For the choice of the weights, one may choose the weight at ω_i to be the absolute value of the CF at the frequency of interest, i.e. $W_i = |\Phi_Z(\omega_i)|$. Since $\Phi_Z(\omega_i)$ is nearly zero for high frequency points, this choice may tend to ignore the optimization for high frequency points. Another second choice would be to devise a weight series that decreases with ω_i but does not diminish significantly for high values of ω_i . One such function would be $W_i = (\log_{10}(\omega_i) + 7)^{-1}$. The two choices for the weight function are referred to as option 1 and option 2, respectively.

Executing the optimization procedure described above in the search for the fixed integral limits \hat{a} and \hat{b} , we obtain the results shown in Table 4.1. The table lists the quasi-optimized integral limits \hat{a} and \hat{b} values for the LGQ rule for each of the three values of N that are used and for both options of the weighting function. The table also lists the corresponding optimized integral limits \check{a} and \check{b} , of course as a function of ω . It can be seen that the weights function used in option 2 produces pairs (\hat{a}, \hat{b}) that are very close to the range of pairs for optimized integral limits (\check{a}, \check{b}) .

Table 4.1: quasi-optimized integral limits for LGQ rule.

Weights function option	Number of quadrature points N	$(\hat{a}, \hat{b}), \sigma = 6 \text{ dB}$		
		$(\hat{a}, \hat{b}), \sigma = 6 \text{ dB}$	$(\hat{a}, \hat{b}), \sigma = 12 \text{ dB}$	
Option 1: $W_i = \Phi_Z(\omega_i) $	10	(-5,5)	(-8,6)	
	25	(-8,7)	(-11,12)	
	45	(-9,8)	(-18,14)	
Option 2: $W_i = (\log_{10}(\omega_i) + 7)^{-1}$	10	(-12,1)	(-18,10)	
	25	(-15,5)	(-18,8)	
	45	(-16,5)	(-19,14)	
Optimized $(\check{a}, \check{b}), \sigma = 12 \text{ dB}$	$\omega = 10^{-3}$	$\omega = 10^0$	$\omega = 10^3$	$\omega = 10^6$
	(-23.72,10.31)	(-23.84,3.59)	(-25.01,-3.21)	(-27.66,-10.04)

Figure 4.4 shows an example of a 3D surface corresponding to the weighted sum of relative errors for one case selected from Table 4.1. The surface corresponds to $N = 10$ quadrature points and utilizes the second weights function.

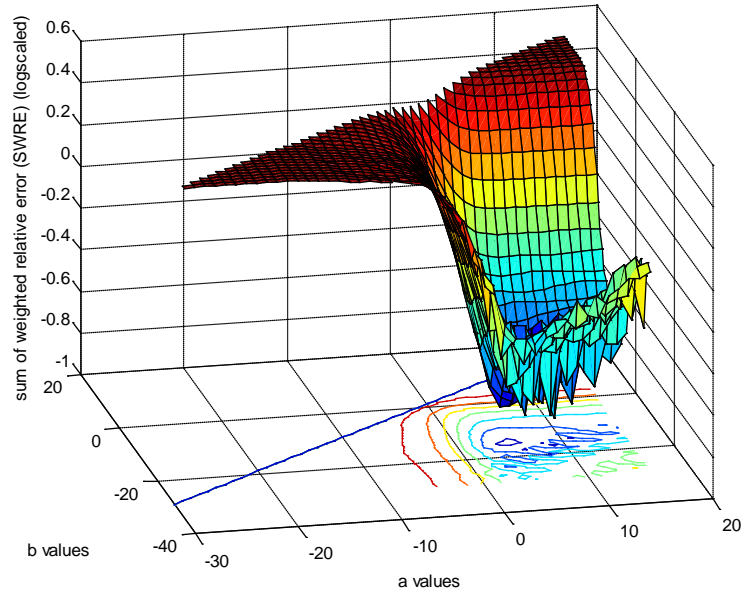


Figure 4.4: Surface for logarithm of weighted sum of relative error for the computation of absolute CF for $\sigma_{\text{dB}} = 12$ dB using the LGQ rule with $N = 10$ as a function integral limits a and b .

Utilizing the quasi optimized integral limits \hat{a} and \hat{b} shown in Table 4.1, the relative error is obtained in a manner similar to that in Figure 4.2 and Figure 4.3. The results are shown in Figure 4.5.

For the LGQ curves, results show some improved accuracy relative to the corresponding curves in Figure 4.3, however, as expected, the relative accuracy is still lower than that for the case of optimized integral limits.

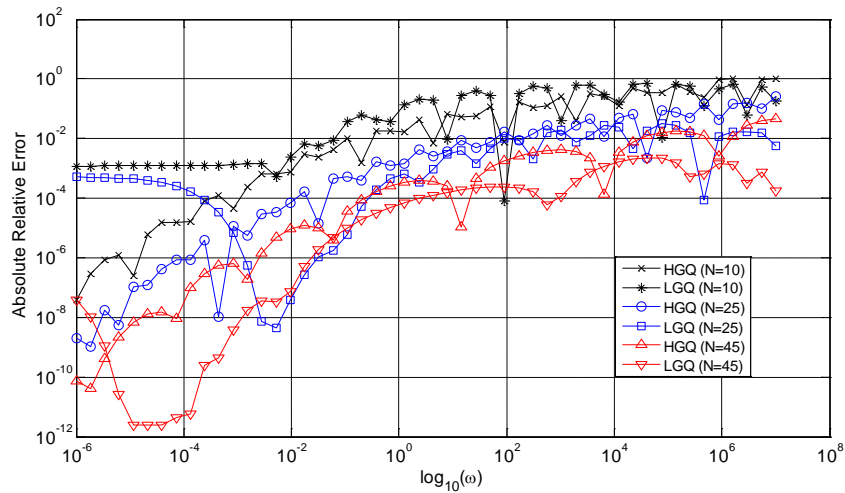


Figure 4.5: Evaluation of relative error for the computation of absolute of CF for $\sigma_{\text{dB}} = 12$ dB using HGQ and LGQ with fixed integral limits \hat{a} and \hat{b} .

While it is clear from the previous table that the quasi-optimized integral limits \hat{a} and \hat{b} are different for different numbers of quadrature points, N , and in a final attempt to simplify the problem even further, one may use a specific pair of \hat{a} and \hat{b} values for the evaluation of the LGQ regardless of N . This makes the derived quasi integral limits a function of the LN RV parameter σ_{dB} and not a parameter related to the computation method. Results obtained using this last method provide less accuracy or higher relative error curves compared to those shown in Figure 4.4. Experiments show that using the pair for the highest N values for the computation results in the most improved accuracy across the other values of N .

4.3 Utilization of LGQ with Optimized Limit in Computing CDF of Sum of Independent LN RVs

In this subsection, we utilize the new expression derived for the approximate CF specified by the relation (4.4) in computing the CDF for the sum of independent LN RVs. The objective is to compare the resulting CDF when the LGQ rule is used to compute the CF of the individual RVs with that obtained with the HGQ rule used previously.

While the derived results are applicable to the case of independent and non-identical RVs, the evaluations here focus on the IID case only for simplicity. For the sum W of IID K LN RVs with a specific σ_{dB} parameter, the CF $\Phi_W(\omega)$ is simply the CF of the individual RV or its approximation, $\tilde{\Phi}_Z(\omega)$, raised to the K^{th} power. Here we utilize (4.4) to evaluate $\tilde{\Phi}_Z(\omega)$. To evaluate the CDF of W , we utilize the approach developed in Section 3.2. Specifically, we apply (3.5) after the change of variables and approximate the integral with three different quadrature rules employed therein, namely the Clenshaw-Curtis (CC), Fejer2, and Legendre. Figures 4.6 and 4.7 show the results of plotting the CDF of the sum of $K=20$ IID lognormal RVs with optimized integral limits \check{a} and \check{b} and also quasi-optimized integral limits \hat{a} and \hat{b} , respectively.

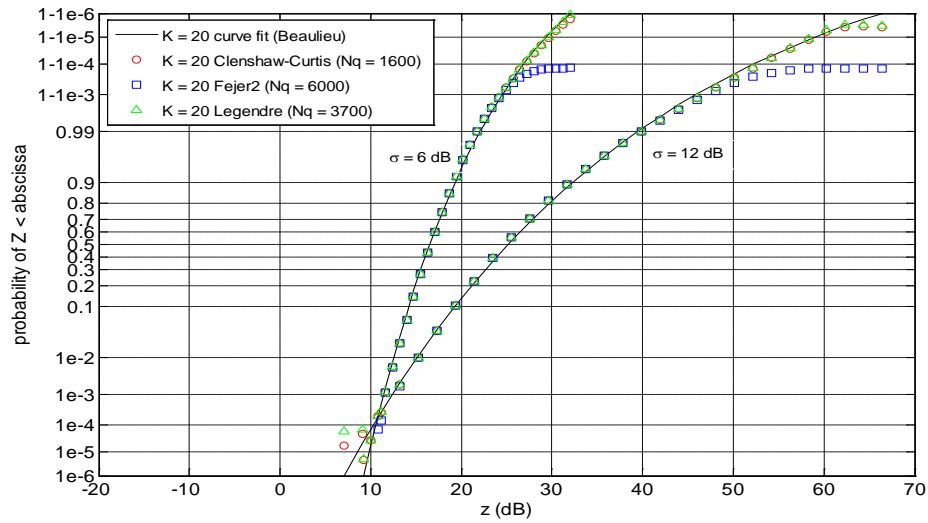


Figure 4.6: The CDF of the sum of $K=20$ IID lognormal RVs $\mu_{\text{dB}}=0\text{dB}$ and $\sigma_{\text{dB}}=6$ and 12 dB using the curve fit in [35] and three quadrature rules: Clenshaw-Curtis, Fejer2, and Legendre, with optimized integral limits \check{a} and \check{b} for LGQ approach.

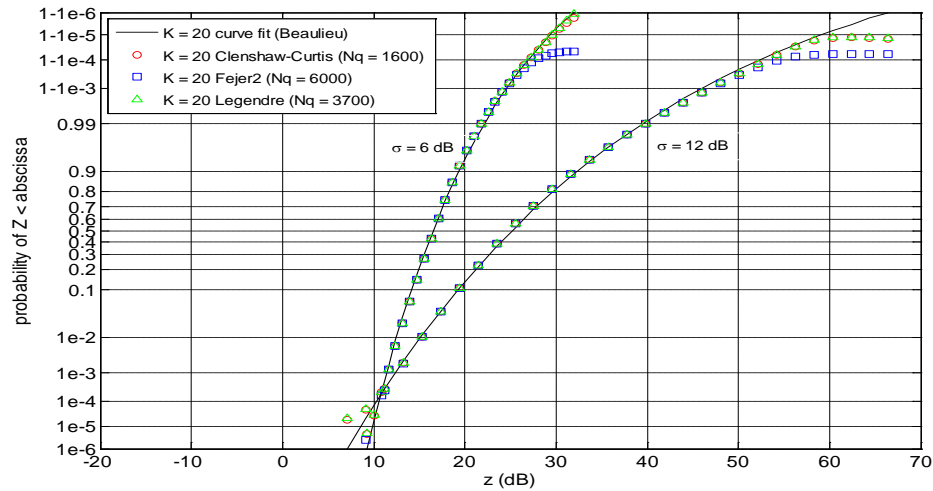


Figure 4.7: The CDF of the sum of $K=20$ IID lognormal RVs $\mu_{\text{dB}}=0\text{dB}$ and $\sigma_{\text{dB}}=6$ and 12 dB using the curve fit in [35] and three quadrature rules: Clenshaw-Curtis, Fejer2, and Legendre, with quasi-optimized integral limits \hat{a} and \hat{b} for LGQ approach.

Chapter 5

APPLICATION TO CDMA DATA NETWORK

This chapter attempts to utilize the developed methods for computing the CDF for the sum of LN RVs to provide an expression for the CDF of the cell site traffic power for a direct-sequence code division multiple access (DS-CDMA) system. In the material that follows, we first introduce the problem of computing the distribution of cell site traffic power and then provide the development leading to the desired result using the methods presented in earlier chapters.

5.1 Background Material

At the core of radio resource management procedures for DS-CDMA system, is a formulation that relates the quality of the wireless link, as reflected by the achieved energy-per bit to noise power spectral density ratio E_b/N_0 and the status of the system in terms of granted connections speeds, system bandwidth, RF propagation conditions, and other network-related parameters. Assume a cellular DS-CDMA with arbitrary frequency reuse factor supporting arbitrary Q discrete service bit rates given by the set $V = \{R_0, R_1, \dots, R_{Q-1}\}$. Let the cell of interest be denoted by cell 0, while the co-channel interferers be numbered from 1 onwards. When K connections (calls or data bursts) are to be supported by the system where the k^{th} burst is assigned the bit rate r_k , then the corresponding link quality for the k^{th} burst is given by:

$$\left[\frac{E_b}{N_0}\right]_k = \frac{BW}{r_k} \times \frac{P_k L_{k0} 10^{\zeta_{k0}/10}}{(1 - \rho) L_{k0} 10^{\zeta_{k0}/10} \left[\sum_{l=0, l \neq k}^{K-1} P_l + P_{ov}\right] + P_T \times \sum_{\forall m} L_{km} 10^{\zeta_{km}/10}} \quad 5.1$$

where BW is the system bandwidth, L_{km} and ζ_{km} are the path loss coefficient and the shadowing factor, respectively, between the k^{th} user in the cell of interest, and the m^{th} cell site for $m = 0, 1, 2, \dots$. The relation in (5.1) assumes the resource management procedure operating in the cell site of interest allocates an amount of power, P_k Watts, for the k^{th} connection. The path loss coefficient L_{km} depends on the model applicable for the system, while the shadowing factor ζ_{km} is a Gaussian random variable with zero mean and a standard deviation equal to σ_{dB} , a parameter reflecting the severity of the shadowing process.

The power allocated to overhead channels is given by $P_{ov} = \beta P_T$, where $0 < \beta < 1$, and P_T is the total transmit power for the cell site. This means $(1 - \beta)P_T$ is the power limit for all traffic transmissions. In addition, the formula (5.1) conservatively assumes each co-channel cell is transmitting at the total cell site power, P_T , and that an orthogonality factor $0 < \rho < 1$ is used to control the severity of the intracell interference.

Fig. 5.1 depicts the cellular configuration used for the cell-site traffic power problem. This figure shows the cell of interest where users are located randomly and also the first tier of 6 co-channel interferers. The second tier of co-channel interferers would be a second ring of twice the radius of the first ring and with cells numbered from 7 to 18. Cells belonging to the second tier are not shown in Fig. 5.1.

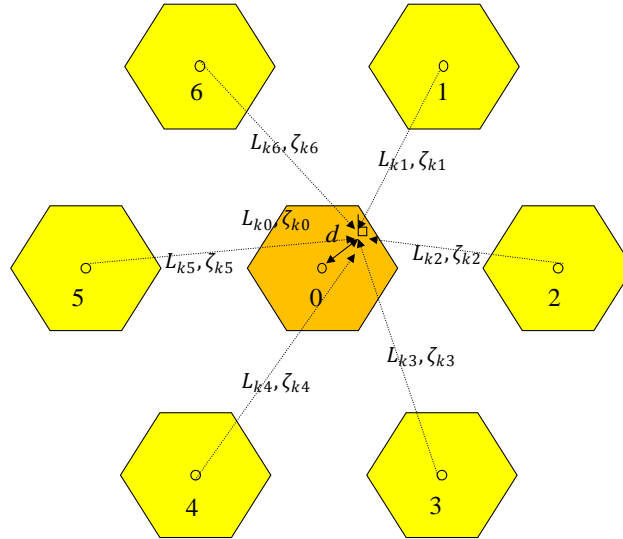


Figure 5.1: Cellular configuration for cell-site traffic power problem showing cell of interest, numbered cell 0, and cells belonging to first tier of co-channel interferers numbered 1 to 6. Cells belonging to second tier of co-channel interferers numbered 7 to 18 are not shown.

An important quantity for resource management procedures is the sum of downlink traffic power. The work in [57] have shown that using (5.1), the sum of traffic powers, $\sum_{k=0}^{K-1} P_k$, can be given by:

$$\sum_{k=0}^{K-1} P_k = P_T \frac{\beta \sum_{k=0}^{K-1} G_k + \frac{1}{1-\rho} \sum_{k=0}^{K-1} G_k f_k}{1 - \sum_{k=0}^{K-1} G_k} \quad 5.2$$

where $G_k = g_k / (1 + g_k)$ and $g_k = (E_b/N_0)_{\min} / (BW/r_k)(1 - \rho)$. The parameter f_k is the ratio of the sum of signal attenuation factors (path loss times the shadowing factor) from all interfering cell sites to the attenuation factor related the cell of interest. The parameter f_k is given by:

$$f_k = \frac{\sum_{\forall m} L_{km} 10^{\zeta_{km}/10}}{L_{k0} 10^{\zeta_{k0}/10}} \quad 5.3$$

for $k = 0, 1, 2, \dots, K - 1$. The parameters G_k 's, ρ , P_T , and β in (5.3) are all constants for a particular set of accepted connections in the system, while the only random variable that depends on the users' locations and the RF propagation model is the quantity $\sum_{k=0}^{K-1} G_k f_k$. Therefore to characterize the downlink traffic power $\sum_{k=0}^{K-1} P_k$, it is sufficient to characterize the quantity $\sum_{k=0}^{K-1} G_k f_k$. Let the quantity $\sum_{k=0}^{K-1} P_k$ be denoted by A , while the quantity $\sum_{k=0}^{K-1} G_k f_k$ be denoted by B . It is clear from (5.3) that A is a linear transformation of the random variable B . That is, $A = c_1 B + c_2$, where the constants c_1 and c_2 are given by $\frac{P_T(1-\rho)^{-1}}{1-\sum_{k=0}^{K-1} G_k}$ and $\frac{\beta P_T \sum_{k=0}^{K-1} G_k}{1-\sum_{k=0}^{K-1} G_k}$, respectively. Therefore, the cumulative probability distribution function (CDF) for A can be written as

$$F_A(x) = F_B\left(\frac{x - c_2}{c_1}\right) \quad 5.4$$

where $F_B(x)$ is the CDF for the variable B . One can write an equivalent relation $f_A(x) = \frac{1}{c_1} f_B\left(\frac{x-c_2}{c_1}\right)$ relating the PDF for the quantity A , $f_A(x)$, to the PDF for B , $f_B(x)$. Therefore, it is sufficient to compute the PDF or CDF for the variable B in order to completely specify the distribution for A . The quantity B is a weighted sum of the independent random variables f_k 's specified by (5.3). There is no known closed form formula to calculate the probability distribution for f_k , and therefore there is no known closed form formula for the distribution $f_B(x)$ that characterizes the quantity $\sum_{k=0}^{K-1} G_k f_k$.

Earlier developments in [58] have shown that the empirical distribution of the RV f_k is similar to a lognormal RV. Therefore, our problem is transformed to one of computing

the distribution for the sum of independent but not identical lognormal-like variables. This thesis work will attempt to utilize methods and experience developed for computing the distribution of sum of lognormal RVs in estimating the distribution for the quantity $B = \sum_{k=0}^{K-1} G_k f_k$, and subsequently, the distribution of the sum of traffic power specified by $A = \sum_{k=0}^{K-1} P_k$.

5.2 Parameterization of the Distribution of f_k

Considering the cellular system configuration outlined in section 5.1 and following the same steps as in [58] we generate the empirical distribution of the random variable f_k for different values of the path loss exponent α and the shadowing spread σ_{dB} . However, for this thesis work, we impose the usage of standard hexagonal cells with cell radius normalized to one kilometer. It should be noticed that the path loss exponent and the shadowing spread are characteristics of the propagation environment and not the cellular system configuration. The remaining parameters appearing in relation (5.1) such as total power budget P_T , fraction of overhead power β , orthogonality factor ρ , bandwidth BW , the acceptable signal quality E_b/N_0 , and system rates $\{R_0, R_1, \dots, R_{Q-1}\}$, are all technology-dependent and represent the cellular system configuration.

The empirical distribution for the RV f_k is shown in Fig. 5.2 using markers for values of the path loss exponent α that range from 0 to 6 and a shadowing spread ranging from 6 dB to 12 dB. Low values of path loss exponent are typical for open rural areas while high values are typical of indoor propagation environments. With respect to the shadowing spread σ_{dB} , it is high for highly obstructed and shadowed areas and low

otherwise. The empirical distribution is obtained by evaluating relation (5.3) for an excessive number of uniform random locations of subscribers in the cell of interest. For each subscriber location, the path loss gains L_{km} 's and shadowing factors ζ_{km} 's with respect to each of the cell of interest, i.e. cell 0, and the surrounding 18 co-channel cells numbered 1 through 18 are evaluated and then the f_k sample is computed. The process is repeated for 5×10^6 times for the same α and σ_{dB} values to yield the CDF plots shown in Fig. 5.2. The high number of iterations is required to obtain CDF values as low as 10^{-6} and as high as $(1 - 10^{-6})$.

The previous figure plots the distribution for the RV f_k on a normal probability paper. It can be noticed that the markers plots are very close to straight lines for a given pair of α and σ_{dB} . Therefore, one may approximate the f_k RV for a given pair of α and σ_{dB} with lognormal RV with specific parameters $\hat{\mu}$ and $\hat{\sigma}$. That is

$$f_k \sim \text{LN}(\hat{\mu}, \hat{\sigma}) \quad 5.5$$

The parameters $\hat{\mu}$ and $\hat{\sigma}$ for the LN RV may be obtained by matching the mean and the standard deviation to those of the original f_k RV. The model specified in relation (5.5) replaces the propagation environment parameters α and σ_{dB} with specific values for $\hat{\mu}$ and $\hat{\sigma}$ for the equivalent lognormal RV. For the range of interest of the path loss exponent and shadowing spread values, Table 5.1 lists the corresponding $\hat{\mu}$ and $\hat{\sigma}$ values for the equivalent lognormal RV.

Having identified that the distribution of the RV f_k may be approximated by a lognormal RV with parameters $\hat{\mu}$ and $\hat{\sigma}$ that are function of the path loss exponent α and

the shadowing spread σ_{dB} , then the problem of computing the CDF for the quantity $B = \sum_{k=0}^{K-1} G_k f_k$ reduces to one of computing the CDF for the sum of non-identical and independent lognormal RVs. It should be noted that for the same α and σ_{dB} values, all f_k 's are independent and identically distributed. The scaling with the parameter G_k , which may be different from one k^{th} connection to the next, transforms the problem into a sum of non-identical and independent RVs.

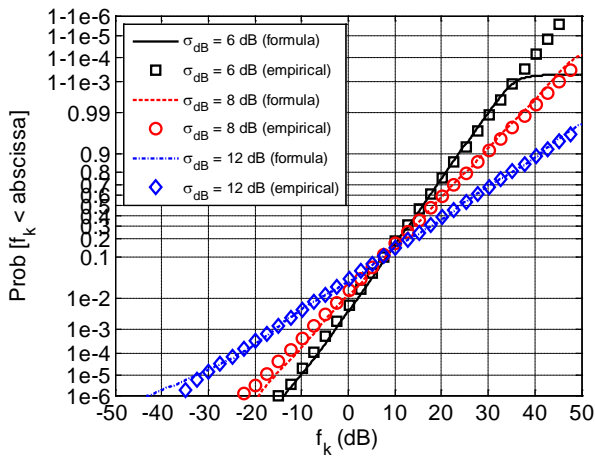
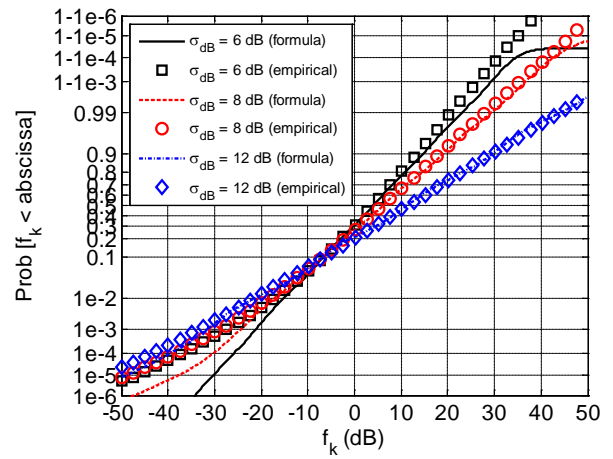
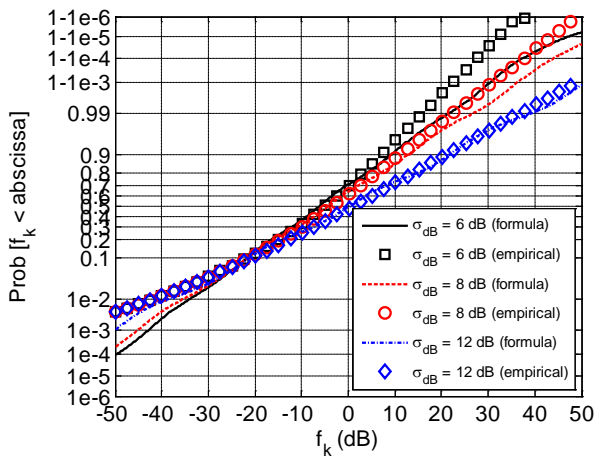
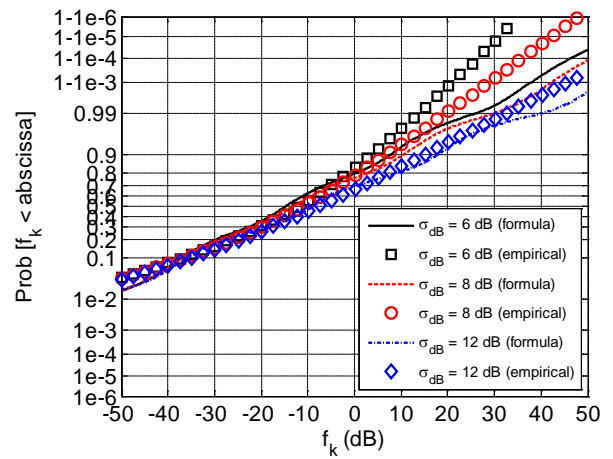
a) path loss exponent $\alpha = 0$ b) path loss exponent $\alpha = 2$ c) path loss exponent $\alpha = 4$ d) path loss exponent $\alpha = 6$

Figure 5.2: Distribution function for RV f_k evaluated using Monte-Carlo simulations or using the new expression with $N = 5$ for different values of path loss exponent α and shadowing spread σ_{dB} . The simulation results are shown using markers while the new expression results are plotted as lines.

Table 5.1: Approximation for f_k RV and parameters $\hat{\mu}$ and $\hat{\sigma}$ for equivalent LN RV.

Path loss exponent, α	Shadowing spread, σ_{dB}	Lognormal (Matching)	
		$\hat{\mu} = E[\ln(f_k)]$	$\hat{\sigma} = \sqrt{\text{Var}[\ln(f_k)]}$
0	6	3.670	1.459
	8	4.238	1.972
	12	5.582	3.023
2	6	0.831	1.819
	8	1.367	2.256
	12	2.658	3.216
4	6	-1.470	2.717
	8	-1.022	3.025
	12	0.110	3.783
6	6	-3.383	3.854
	8	-3.027	4.062
	12	-2.091	4.634

5.3 Developed Expressions for $F_B(x)$ and $F_A(x)$

Using the relation (5.5) and the material developed in [14] and cited in subsection 1.2.2, the approximate CF for the RV f_k can be written as

$$\tilde{\Phi}_{f_k}(\omega) = \sum_{n=1}^N A_n e^{-a_n \omega} \quad (5.6)$$

where the coefficients A_n and a_n are given by $c w_n \exp[-j\pi d_n / (\sqrt{2}\hat{\sigma})]$ and $\exp[\sqrt{2}\hat{\sigma}d_n + \hat{\mu}]$, respectively. w_n and d_n are the N -points HGQ weights and nodes as tabulated in [21]. The constant j is equal to $\sqrt{-1}$ while the constant c is equal to $\exp[\pi / (2\sqrt{2}\hat{\sigma})^2] / \sqrt{\pi}$.

Figure 5.2 also shows the CDF of the equivalent LN RV, shown in lines as opposed to markers, with the identified $\hat{\mu}$ and $\hat{\sigma}$ (taken from Table 5.1) that correspond to the respective path loss exponent and shadowing spread values. The CDF is not evaluated using the conventional formula specified by relation (1.6) but rather using relation (1.22) with the utilization of the coefficients A_n and a_n computed for (5.6). The shown CDFs in Figure 5.2 are evaluated for $N = 5$ HGQ weights and nodes. It can be observed that the new formula for the distribution of f_k reasonably matches the empirical results even for a value of N as low as 5. More accurate results are possible with N greater than 5.

Correspondingly, the CF for the scaled RV $G_k f_k$, denoted by $\tilde{\Phi}_{G_k f_k}(\omega)$, may be computed in terms of $\tilde{\Phi}_{f_k}(\omega)$ as $\tilde{\Phi}_{f_k}(G_k \omega)$. Therefore, the CF function of the summation $B = \sum_{k=0}^{K-1} G_k f_k$ where f_k 's are independent RVs, is simply given by:

$$\tilde{\Phi}_B(\omega) = \prod_{k=0}^{K-1} \tilde{\Phi}_{G_k f_k}(\omega) = \prod_{k=0}^{K-1} \tilde{\Phi}_{f_k}(G_k \omega) \quad (5.7)$$

since $\tilde{\Phi}_{f_k}$ is written in the form of a sum of weighted exponentials as in (5.6), then one can expand (5.7) to be also of the form of sum of weighted exponentials. That is the CF $\tilde{\Phi}_B(\omega)$ may be written as:

$$\tilde{\Phi}_B(\omega) = \sum_{m=1}^M A_m^{(B)} e^{-a_m^{(B)} \omega} \quad (5.8)$$

where the coefficients $A_m^{(B)}$ and $a_m^{(B)}$ are obtained by performing the multiplication of the K individual CFs in (5.7). The number of terms M in (5.8) is generally upper bounded by N^K . Now the CDF for the quantity B is readily computed using:

$$\tilde{F}_B(x) = \text{Re} \left\{ \frac{j}{\pi} \sum_{m=1}^M A_m^{(B)} \ln \left(a_m^{(B)} / (jx + a_m^{(B)}) \right) \right\} \quad (5.9)$$

similar to the result in relation (1.22). Finally, the target CDF for the sum of traffic powers $A = \sum_{k=0}^{K-1} P_k$ is simply given by:

$$\tilde{F}_A(x) = \text{Re} \left\{ \frac{j}{\pi} \sum_{m=1}^M A_m^{(B)} \ln \left(a_m^{(B)} / (j(x - c_2)/c_1 + a_m^{(B)}) \right) \right\} \quad (5.10)$$

where the constants c_1 and c_2 are as defined as for relation (5.4).

The above result shown in (5.10) specifies the new formula for computing the distribution of cell site traffic power for a CDMA data network. It presents an approximate closed-form alternative expression for obtaining the distribution $\tilde{F}_A(x)$ using Monte-Carlo simulations.

One direct consequence of using the formula in (5.10) is the ability to compute the probability of power outage, denoted by P_{out} , for the CDMA network. If P_{out} is defined as the probability that the traffic power needed to support the K connections exceeds the maximum possible $(1 - \beta)P_T$, then substituting in (5.10) we obtain:

$$\begin{aligned}
 P_{out} &= 1 - \tilde{F}_A((1 - \beta)P_T) \\
 &= 1 - \operatorname{Re} \left\{ \frac{j}{\pi} \sum_{m=1}^M A_m^{(B)} \ln \left(a_m^{(B)} / \left(j((1 - \beta)P_T - c_2)/c_1 + a_m^{(B)} \right) \right) \right\} \quad (5.11)
 \end{aligned}$$

The formulas (5.9), (5.10), and (5.11) are the main results in this chapter.

5.4 Numerical Results

To evaluate the above formulas and provide numerical examples, we consider a 3rd generation wireless cellular WCDMA systems. The channel bandwidth for the system is equal to 5 MHz while the supported data rates set, V is equal to {32, 64, 128, 256, 384} kilobits per second. The total cell site power budget P_T is taken to be 24 Watts while 20% of this is allocated for overhead channels. This means only a maximum of 19.2 Watts can be allocated for traffic connections in a cell site. The orthogonality parameter ρ is equal to 0.1. The overall system parameters and their default values are listed in Table 5.2.

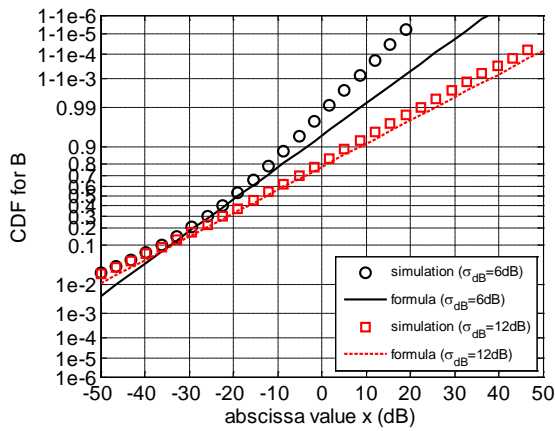
Table 5.2: Simulation parameters used for WCDMA system.

Parameter	Value	Remark
bandwidth, W	5 MHz	channel bandwidth for WCDMA system
total power, P_T	24 Watts	total cell site power budget
Fraction of overhead power, β	0.2	fraction of cell site power allocated for overhead channel
minimum signal quality, E_b/N_0	10 dB	minimum energy per bit relative to noise power spectral density required for proper signal reception
orthogonality parameter, ρ	0.1	parameter specifying intracell interference power
systems rates, V	32, 64, 128, 256, and 384 kb/s	service rates supported by system

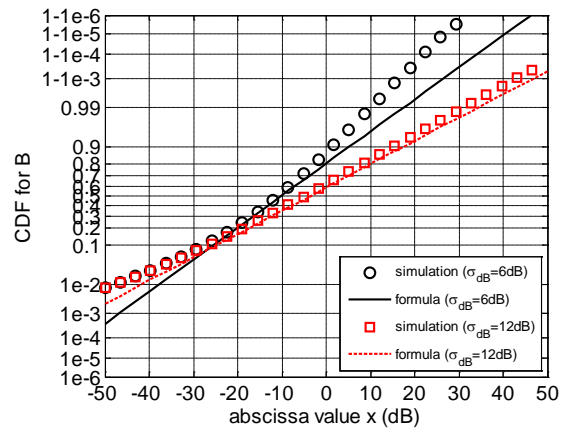
For the evaluation of the formulas we need to assume the existence of K ongoing connections where the subscribers are located randomly in the cell of interest, each with some assigned system rate. Let the system state be defined by the state $(n_0, n_1, \dots, n_{Q-1})$ where n_q for $q = 0, 1, \dots, Q - 1$ is the number of connections using the q^{th} system rate. For the system parameters shown above, Q is equal to 5. The total number of connections K is equal to $\sum_{q=0}^{Q-1} n_q$. It is clear from relation (5.2) that not all system states are feasible or possible to support. Only states where $\sum_{k=0}^{K-1} G_k$ is less than 1 can be supported by the system. For states where $\sum_{k=0}^{K-1} G_k > 1$, the entire system traffic power is not sufficient to support the connections specified in the respective states. This can also be inferred from equation (5.2) as the sum of traffic powers must be a positive quantity.

We first evaluate the CDF of the RV variable $B = \sum_{k=0}^{K-1} G_k f_k$ using relation (5.9). For simulation purposes, we employ 5×10^6 samples of RV to plot the empirical CDF while we use $N = 15$ points for the HGQ rule used to approximate the CF for the RV f_k . Fig. 5.3 shows the CDF for the RV $B = \sum_{k=0}^{K-1} G_k f_k$ for path loss exponent equal to 4 and two values of the shadowing spread parameter σ_{dB} : 6 dB and 12 dB. The evaluation is chosen for 4 distinct states: state 1 = (1, 0, 0, 0, 0), state 2 = (0, 0, 0, 0, 1), state 3 = (1, 1, 0, 1, 1), and state 4 = (0, 2, 0, 1, 1). The first two states represent the simple case of only one connection existing in the system, while the third and fourth states represent the cases of heterogeneous connections. The selected four states are feasible and the corresponding $\sum_{k=0}^{K-1} G_k$'s for the specified connections are equal to 0.055, 0.409, 0.882, and 0.931, respectively.

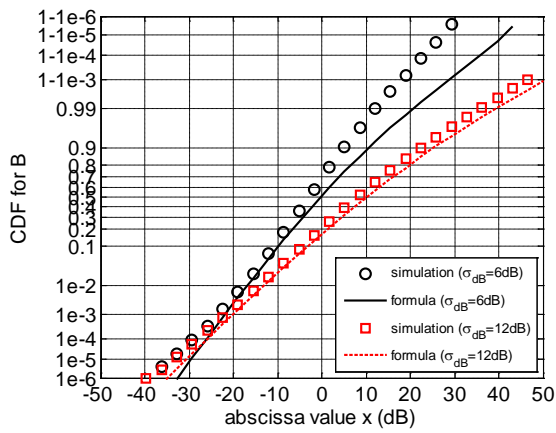
It can be observed that the formula approximates the empirical CDF well especially for low values of the abscissa. Furthermore, the approximation seems to improve as the value for the shadowing spread σ_{dB} increases. The shown cases for the 4 states correspond to cases of a system which is progressively loaded where the load is proportional to the $\sum_{k=0}^{K-1} G_k$. For each of the selected states, we use formula (5.11) to compute the probability of power outage. The results are shown in Fig. 5.4 in the form of bar charts. Again, we note that simulation results are very well approximated by the new formula. The outage probabilities for the case of $\sigma_{\text{dB}} = 6$ dB are lower than those for $\sigma_{\text{dB}} = 12$ dB. The outage probability for the last two states correspond to almost 100% outage.



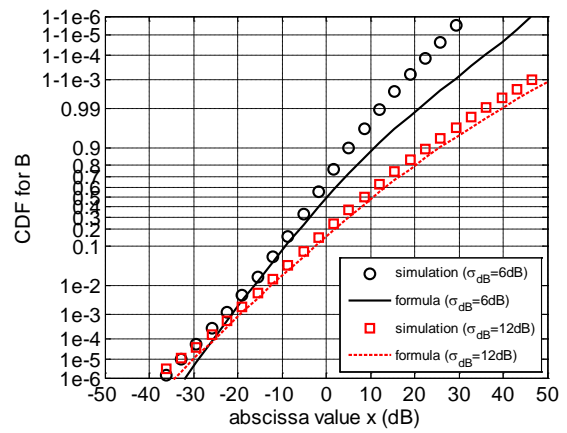
$$\text{State 1} = (1, 0, 0, 0, 0) - \sum_{k=0}^{K-1} G_k = 0.055$$



$$\text{State 2} = (0, 0, 0, 0, 1) - \sum_{k=0}^{K-1} G_k = 0.409$$



$$\text{State 3} = (1, 1, 0, 1, 1) - \sum_{k=0}^{K-1} G_k = 0.882$$



$$\text{State 4} = (0, 2, 0, 1, 1) - \sum_{k=0}^{K-1} G_k = 0.931$$

Figure 5.3: CDF plots for RV $B = \sum_{k=0}^{K-1} G_k f_k$ for path loss exponent equal to 4 and two shadowing spread values (6 dB and 12 dB).

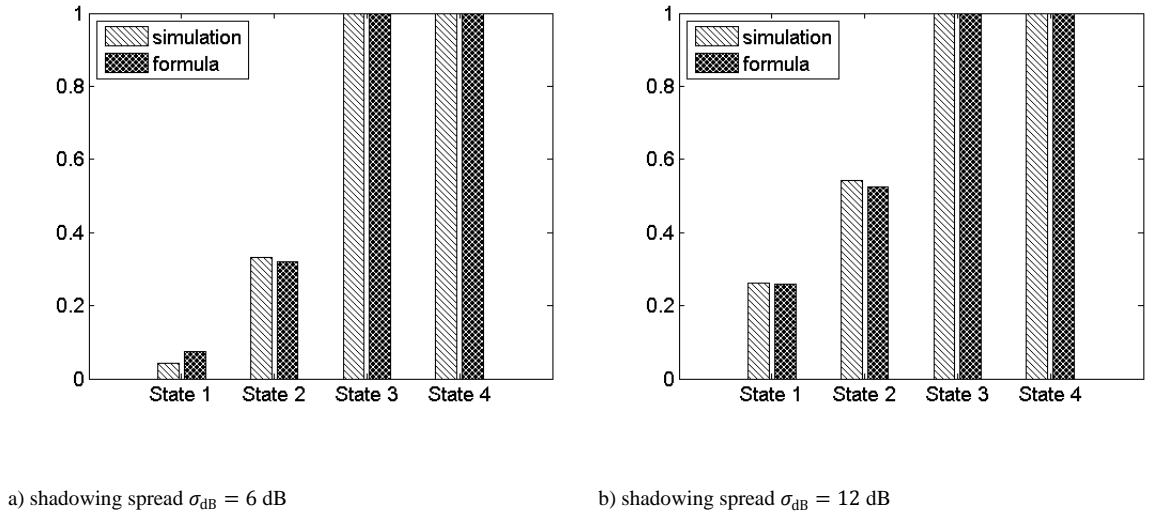


Figure 5.4: Probability of power outage for the four selected states: state 1 = (1, 0, 0, 0, 0), state 2 = (0, 0, 0, 0, 1), state 3 = (1, 1, 0, 1, 1), and state 4 (0, 2, 0, 1, 1).

Finally, we evaluate the outage probabilities for a group of states specified by $(n_0, n_1, \dots, n_{Q-1})$ where we allow the number of connections, n_q , of one specific system rate, say R_q for $q \in \{0, 1, 2, \dots, Q-1\}$, to increase from zero to the maximum possible number of connections that can be supported. We plot the power outage probability versus the number of connections. Fig. 5.5 shows the outage probabilities for different mixtures of connection rates, where the number of connections for one specific service rate is allowed to increase progressively. The outage probabilities are again shown for the case of path loss exponent of 4 and two shadowing spread values of $\sigma_{\text{dB}} = 6$ dB and $\sigma_{\text{dB}} = 12$ dB. The four plots use the same plot limits for the x -axis and y -axis for ease of comparison. As the quantity $\sum_{k=0}^{K-1} G_k$ for the states in a particular outage plot approaches unity, the states become infeasible and the outage probability approaches one.

Again, consistent with previous observations, the outage probability for $\sigma_{dB} = 12$ dB is higher than that for $\sigma_{dB} = 6$ dB. Furthermore, the approximation presented by the formula improves with the increase of the shadowing spread factor or the number of connections.

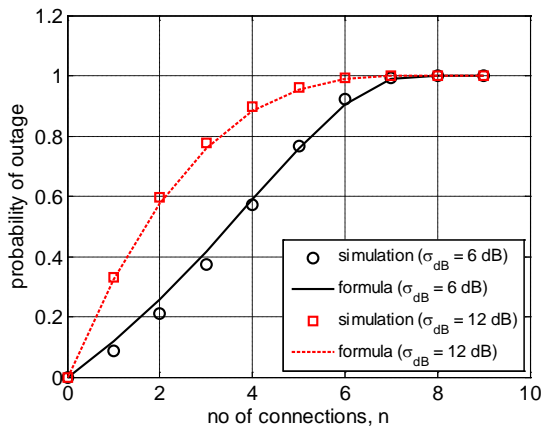
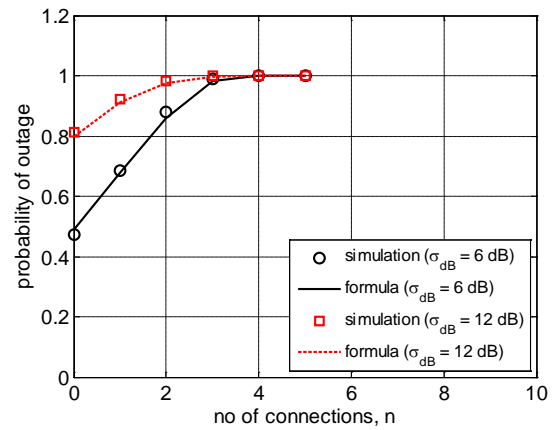
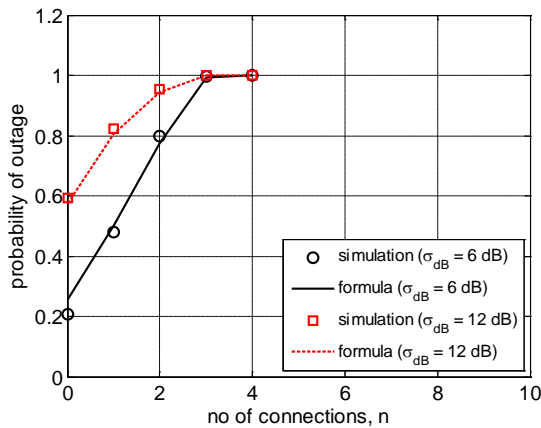
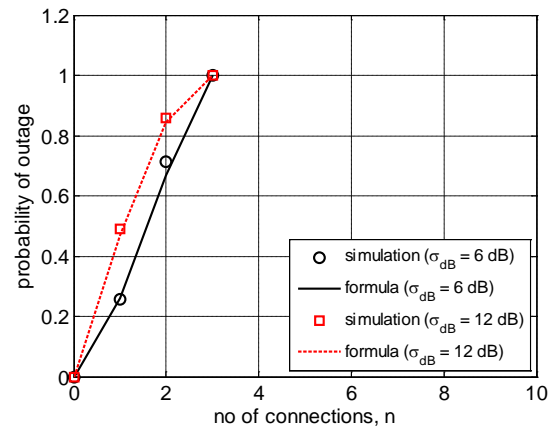
a) States $(0, n, 0, 0, 0)$ b) States $(2, n, 0, 1, 0)$;c) States $(0, 2, n, 0, 0)$ d) States $(0, 0, 0, n, 0)$;

Figure 5.5: Power outage probability as a function of number of connections for a specific mixture of connection rates for a path loss exponent of 4 and a shadowing spread of 6 dB and 12 dB.

Chapter 6

CONCLUSION AND FUTURE DIRECTIONS

This chapter presents the main conclusions resulting from the thesis work and also highlights some of the possible future directions.

6.1 CONCLUSIONS

The problem of characterizing the sum of lognormal random variables is of interest in variety of fields in science and engineering. The problem is still open as most if not all of the proposed solutions found in the literature are suitable or applicable for only limited scenarios. This thesis work initially intended to build on the work in [14] and exploit the newly found formula for the characteristic function specified by (1.19), in its unexpanded form, to enhance the computation accuracy for the CDF for the case of the sum of independent and identically distributed lognormal random variables.

Along the main objective, the work in Chapter 3 presents formulas for computing the CDF for the sum of independent and identically distributed lognormal RVs using quadrature rules specialized for oscillatory integrands, namely, Clenshaw-Curtis, Fejr2, and also using the Legendre-Gauss quadrature rule. These formulas perform change of variables prior to evaluating the integration using the respective quadrature rule to reduce the severity of the oscillation. In another contribution, we showed an application of the Epsilon algorithm to approximate the integral using a smaller number of partial sums to arrive at the value of the original sum. The corresponding chapter displays results for

evaluating the CDF for extreme cases such as the case of 20 IID lognormal RVs with $\sigma_{\text{dB}} = 12$ dB. The used methods show some enhancements for the CDF computation near the lower and upper tail of the distribution with the best performance attributed to the Clenshaw-Curtis (CC) and the Legendre-Gauss quadrature rules. The CC quadrature rule was able to compute the CDF with a number of weights and nodes equal to 1600 and achieve minimum relative error. Using the epsilon algorithm the CDF may be evaluated with as few as 14 partial sums for the extreme points on the abscissa.

The original formula for the CF corresponding to the sum of IID lognormal RVs, at the core of the above development, utilizes the Hermite-Gauss quadrature (HGQ) rule. The work in Chapter 4 attempts to create an alternative formula utilizing the Legendre-Gauss quadrature (LGQ) rule that may require fewer terms for the same level of accuracy as for the HGQ. This Chapter proposes a measure of relative error to assess the accuracy of the proposed computation methods. While the initial implementation of the LGQ requires relatively more computations compared to the original HGQ in terms of computing the optimal integration limits $[\check{a}, \check{b}]$ for each frequency point ω , it produces lower relative errors for the same number of terms. Results show that the LGQ rule with $N = 25$ points achieves lower relative errors ($\sim 10^{-5}$) than the HGQ rule with $N = 45$ points. To alleviate the requirement of having to use different integral limit for different frequencies, we unified the integration intervals for all frequency points to be of the form of $[a^*, b^*]$ where we chose a^* to be equal to the minimum of all possible \check{a} 's while b^* equals the maximum of all possible \check{b} 's. While this approach allows the CF to be expressed in a simple sum of weighted exponentials similar to the case of the HGQ rule, it does not produce results with higher accuracy relative to the original HGQ rule.

Finally, as a compromise, we define and compute quasi-optimal integral limits $[\hat{a}, \hat{b}]$ that produce the lowest weighted relative error for a given number of terms N and σ_{dB} parameter for the LN RVs. Relative error results for the quasi-optimal integral limits are comparable to those obtained for the HGQ rule for the same number of quadrature weights and nodes N .

Lastly, in Chapter 5 we utilize the knowledge of computing the CDF for a sum of independent LN RVs to a resource management problem for a DS-CDMA data system. The Chapter presents an analytical formulation for the cell site traffic power allocations for data subscribers, where the sum of total traffic power allocations is modeled as a linear transformation of the sum of non-identical but independent lognormal-like RVs. Assuming that our lognormal-like RV may be approximated by lognormal RVs, we derived expressions for the PDF and CDF of the total cell-site traffic power as a function of the other system parameters, and computed the probability of outage for a given mixture of subscriber connections. For validation purposes, this chapter evaluates the derived formulas and plots results using the new expressions using Monte-Carlo simulations.

6.2 FUTURE DIRECTIONS

The following list outlines some of the possible future directions for the current work:

1. The unexpanded expression for the CF for the sum of IID LN RV may be exploited by utilizing the CF to derive expressions for the moments as a function of the individual LN RV parameters μ and σ and the HGQ weights and nodes.

These expressions will serve as a new addition to the literature along the lines of characterizing the sum and may also be used in matching the distribution of the sum to some other known distributions. However, this work remains applicable only to the case of the sum of IID LN RVs.

2. Many of the works found in the literature focus on approximating the distribution of the logarithm of the sum of independent LN RVs. Typically, such works compute the moments for the logarithm of the sum using Monte-Carlo simulations. In this thesis, we outlined formulas for the approximate PDF and CDF of the sum that may be transformed using the logarithm function to compute an approximation for the distribution of logarithm of the sum. The transformed approximations may be used to find expressions to approximate moments for the logarithm of the sum as opposed to obtaining the moments using Monte-Carlo simulations.
3. The relative error curves shown in Fig. 4.2, 4.3, and 4.5 utilize the magnitude of the characteristic function in the calculations for the relative error. However, it was observed the relative error in the calculated imaginary part of the CF is usually higher than that for the real part of the CF for the same frequency point ω . This requires further investigation to identify the root cause for this phenomenon.
4. Finally, one may also attempt to quantify the similarity of the resultant PDFs to that of the Normal RV using methods similar to the one suggested in [59].

REFERENCES

- [1] S. Asmussen and L. Rojas-Nandayapa, "Asymptotics of sums of lognormal random variables with Gaussian copula," *Statistics & Probability Letters*, vol. 78, no. 16, pp. 2709-2714, November 2008.
- [2] M. Romeo, V. Da Costa, and F. Bardou, "Broad distribution effects in sums of lognormal random variables," *The European Physical Journal B-Condensed Matter and Complex Systems*, vol. 32, no. 4, pp. 513-525, May 2003.
- [3] C. Hongliang and S. S. Sapatnekar, "Full-chip analysis of leakage power under process variations, including spatial correlations," in *Proceedings Design Automation Conference, 42nd*, June 2005, pp. 523-528.
- [4] S. F. Altschul, T. L. Madden, A. A. Schäffer, J. Zhang, Z. Zhang, W. Miller, and D. J. Lipman, "Gapped BLAST and PSI-BLAST: a new generation of protein database search programs," *Nucleic acids research*, vol. 25, no. 17, p. 3389, September 1997.
- [5] E. Limpert, W. A. Stahel, and M. Abbt, "Log-normal distributions across the sciences: keys and clues," *BioScience*, vol. 51, no. 5, pp. 341-352, May 2001.
- [6] M. Pratesi, F. Santucci, and F. Graziosi, "Generalized moment matching for the linear combination of lognormal RVs: application to outage analysis in wireless systems," *IEEE Transactions on Wireless Communications*, , vol. 5, no. 5, pp. 1122-1132, May 2006.
- [7] S. S. Szyszkowicz, "Interference in cellular networks: sum of lognormals modeling," M.S thesis, Department of Systems and Computer Engineering, Carleton University, Ottawa, Ontario, Canada, January 2007.

- [8] Y. S. Yeh and S. Schwartz, "Outage probability in mobile telephony due to multiple log-normal interferers," *IEEE Transactions on Communications*, vol. 32, no. 4, pp. 380-388, April 1984.
- [9] R. Barakat, "Sums of independent lognormally distributed random variables," *JOSA*, vol. 66, no. 3, pp. 211-216, 1 May 1976.
- [10] M. A. Milevsky and S. E. Posner, "Asian options, the sum of lognormals, and the reciprocal gamma distribution," *Journal of financial and quantitative analysis*, vol. 33, no. 3, September 1998.
- [11] R. B. Leipnik, "On lognormal random variables: I-the characteristic function," *The Journal of the Australian Mathematical Society. Series B. Applied Mathematics*, vol. 32, no. 3, pp. 327-347, January 1991.
- [12] S. Asmussen and L. Rojas-Nandayapa, "Sums of dependent lognormal random variables: asymptotics and simulation," *Preprint*, December 2005.
- [13] D. Cox, "Cochannel interference considerations in frequency reuse small-coverage-area radio systems," *IEEE Transactions on Communications*, vol. 30, no. 1, pp. 135-142, January 1982.
- [14] A. S. H. Mahmoud, "New Quadrature-Based Approximations for the Characteristic Function and the Distribution Function of Sums of Lognormal Random Variables," *IEEE Transactions on Vehicular Technology*, vol. 59, no. 7, pp. 3364-3372, September 2010.
- [15] C. Tellambura and D. Senaratne, "Accurate computation of the MGF of the lognormal distribution and its application to sum of lognormals," *IEEE Transactions on Communications*, vol. 58, no. 5, pp. 1568-1577, May 2010.

- [16] T. S. Rappaport, *Wireless Communications Principles and Practice*: Prentice Hall PTR, Upper Saddle River, NJ, USA, 2nd edition, 2002.
- [17] N. C. Beaulieu, A. A. Abu-Dayya, and P. J. McLane, "Estimating the distribution of a sum of independent lognormal random variables," *IEEE Transactions on Communications*, vol. 43, no. 12, p. 2869, December 1995.
- [18] H. Hashemi, "Impulse response modeling of indoor radio propagation channels," *IEEE Journal on Selected Areas in Communications*, vol. 11, no. 7, pp. 967-978, September 1993.
- [19] A. H. Nuttall, "Alternate forms for numerical evaluation of cumulative probability distributions directly from characteristic functions," *Proceedings of the IEEE*, vol. 58, no. 11, pp. 1872-1873, November 1970.
- [20] J. A. Gubner, "A New Formula for Lognormal Characteristic Functions," *IEEE Transactions on Vehicular Technology*, vol. 55, no. 5, pp. 1668-1671, September 2006.
- [21] M. Abramowitz and I. A. Stegun, *Handbook of mathematical functions with formulas, graphs, and mathematical tables*: New York: Dover, 1972, p.890.
- [22] C. L. J. Lam and T. Le-Ngoc, "Log-shifted gamma approximation to lognormal sum distributions," *IEEE Transactions on Vehicular Technology*, vol. 56, no. 4, pp. 2121-2129, July 2007.
- [23] W. Janos, "Tail of the distribution of sums of log-normal variates," *IEEE Transactions on Information Theory*, vol. 16, no. 3, pp. 299-302, May 1970.

- [24] N. C. Beaulieu and Q. Xie, "An optimal lognormal approximation to lognormal sum distributions," *IEEE Transactions on Vehicular Technology*, vol. 53, no. 2, pp. 479-489, March 2004.
- [25] N. B. Mehta, J. Wu, A. F. Molisch, and J. Zhang, "Approximating a sum of random variables with a lognormal," *IEEE Transactions on Wireless Communications*, vol. 6, no. 7, pp. 2690-2699, July 2007.
- [26] M. Di Renzo, F. Graziosi, and F. Santucci, "Approximating the linear combination of log-normal RVs via pearson type IV distribution for UWB performance analysis," *IEEE Transactions on Communications*, vol. 57, no. 2, pp. 388-403, February 2009.
- [27] D. Schleher, "Generalized Gram-Charlier series with application to the sum of log-normal variates (Corresp.)," *IEEE Transactions on Information Theory*, vol. 23, no. 2, pp. 275-280, March 1977.
- [28] L. Fenton, "The sum of log-normal probability distributions in scatter transmission systems," *IRE Transactions on Communications Systems*, vol. 8, no. 1, pp. 57-67, March 1960.
- [29] S. C. Schwartz and Y. S. Yeh, "On the distribution function and moments of power sums with log-normal components," *The Bell System Technical Journal*, vol. 61, no. 7, pp. 1441-1462, September 1982.
- [30] S. Ben Slimane, "Bounds on the distribution of a sum of independent lognormal random variables," *IEEE Transactions on Communications*, vol. 49, no. 6, pp. 975-978, June 2001.

- [31] F. Berggren and S. B. Slimane, "A simple bound on the outage probability with lognormally distributed interferers," *IEEE Communications Letters*, vol. 8, no. 5, pp. 271-273, May 2004.
- [32] Z. Kostic, I. Maric, and X. Wang, "Fundamentals of dynamic frequency hopping in cellular systems," *IEEE Journal on Selected Areas in Communications*, vol. 19, no. 11, pp. 2254-2266, November 2001.
- [33] P. Cardieri and T. S. Rappaport, "Statistics of the sum of lognormal variables in wireless communications," in *Vehicular Technology Conference Proceedings. VTC 2000-Spring Tokyo*, 2000, pp. 1823-1827 vol. 3.
- [34] A. Safak, "Statistical analysis of the power sum of multiple correlated log-normal components," *IEEE Transactions on Vehicular Technology*, vol. 42, no. 1, pp. 58-61, February 1993.
- [35] N. C. Beaulieu and F. Rajwani, "Highly accurate simple closed-form approximations to lognormal sum distributions and densities," *IEEE Communications Letters*, vol. 8, no. 12, pp. 709-711, Dec. 2004.
- [36] Z. Liu, J. Almhana, and R. McGorman, "Approximating lognormal sum distributions with power lognormal distributions," *IEEE Transactions on Vehicular Technology*, vol. 57, no. 4, pp. 2611-2617, July 2008.
- [37] Z. Wu, X. Li, R. Husnay, V. Chakravarthy, and B. Wang, "A novel highly accurate log skew normal approximation method to lognormal sum distributions," in *IEEE Wireless Communications and Networking Conference, WCNC 2009.*, 5-8 April 2009, pp. 1-6.

- [38] Q. Zhang and S. Song, "A systematic procedure for accurately approximating lognormal-sum distributions," *IEEE Transactions on Vehicular Technology*, vol. 57, no. 1, pp. 663-666, January 2008.
- [39] K. Pearson, "Contributions to the mathematical theory of evolution. II. Skew variation in homogeneous material," *Philosophical Transactions of the Royal Society of London. A*, vol. 186, pp. 343-414, January 1895.
- [40] H. Nie and S. Chen, "Lognormal sum approximation with type IV Pearson distribution," *IEEE Communications Letters*, vol. 11, no. 10, pp. 790-792, October 2007.
- [41] Q. Zhang and S. Song, "Model selection and estimation for lognormal sums in Pearson's framework," in *IEEE 63rd Vehicular Technology Conference, 2006. VTC 2006-Spring.*, Vol. 6, 2006, pp. 2823-2827.
- [42] M. Di Renzo, L. Imbriglio, F. Graziosi, and F. Santucci, "Smolyak's algorithm: a simple and accurate framework for the analysis of correlated log-normal power-sums," *IEEE Communications Letters*, vol. 13, no. 9, pp. 673-675, September 2009.
- [43] L. Zhao and J. Ding, "Least squares approximations to lognormal sum distributions," *IEEE Transactions on Vehicular Technology*, vol. 56, no. 2, pp. 991-997, March 2007.
- [44] L. Féjer, "On the infinite sequences arising in the theories of harmonic analysis, of interpolation, and of mechanical quadratures," *Bulletin of the American Mathematical Society*, vol. 39, no. 521-534, p. 198, 1933.
- [45] C. W. Clenshaw and A. R. Curtis, "A method for numerical integration on an automatic computer," *Numerische Mathematik*, vol. 2, no. 1, pp. 197-205, 1960.

- [46] D. Huybrechs and S. Olver, "Highly oscillatory quadrature," *Highly Oscillatory Problems*, Cambridge Univ. Press, Cambridge, pp. 25-50, 2009.
- [47] A. Iserles, S. Nørsett, and S. Olver, "Highly oscillatory quadrature: The story so far," *Numerical Mathematics and Advanced Applications*, pp. 97-118, 2006.
- [48] L. N. Trefethen, "Is Gauss quadrature better than Clenshaw-Curtis?," *SIAM Review*, vol. 50, no. 1, pp. 67-87, 2008.
- [49] J. A. C. Weideman and L. N. Trefethen, "The kink phenomenon in Fejér and Clenshaw-Curtis quadrature," *Numerische Mathematik*, vol. 107, no. 4, pp. 707-727, February 2007.
- [50] P. Favati, G. Lotti, and F. Romani, "Bounds on the error of Fejér and Clenshaw-Curtis type quadrature for analytic functions," *Applied mathematics letters*, vol. 6, no. 6, pp. 3-8, 1993.
- [51] M. Chawla, "Error estimates for the Clenshaw-Curtis quadrature," *Mathematics of Computation*, vol. 22, pp. 651-656, 1968.
- [52] K. Petras, "Gaussian integration of Chebyshev polynomials and analytic functions," *Numerical Algorithms*, vol. 10, no. 1, pp. 187-202, 1995.
- [53] K. Petras, "Gaussian versus optimal integration of analytic functions," *Constructive approximation*, vol. 14, no. 2, pp. 231-245, 1998.
- [54] D. Shanks, "Non-linear transformations of divergent and slowly convergent sequences," *J. Math. Phys.*, vol. 34, pp. 1-42, 1955.
- [55] P. Wynn, "On a device for computing the $e_m(S_n)$ transformation," *Mathematical Tables and Other Aids to Computation*, vol. 10, no. 54, pp. 91-96, 1956.

- [56] MATLAB. [Online]. Available: <http://www.mathworks.com>
- [57] A. Mahmoud, "Transmission Rate Assignment for Downlink For Multi-Rate Wireless CDMA Data Networks," in *The 2007 IEEE International Conference on Signal Processing and Communications (ICSPC 2007)*. Dubai, United Arab Emirates, 24-27 November 2007, pp. 1091-1094.
- [58] A. S. Mahmoud and M. Aabed, "Approximation Techniques For Analytical Characterization Of Downlink Traffic Power For Multi-Service CDMA Networks," in *The 15th IEEE International Conference on Networks, ICON 2007.* , November 2007, pp. 342-347.
- [59] S. Kullback, "The kullback-leibler distance," *The American Statistician*, vol. 41, pp. 340-341, 1987.

VITA

Name: ABDALLAH HASAN RASHED

Place of Birth: Kuwait.

Nationality: Jordanian

Permanent Address: Beit Leed,
Tulkarm,
Palestine.

Telephone: +970-596 484323

Email Address: abd_rashed2000@yahoo.com

Educational Qualification:

M.S (Computer Engineering)

December 2012

King Fahd University of Petroleum and Minerals

Dhahran, Saudi Arabia.

B. Tech. (Computer Engineering)

June 2008

An-Najah National University, Palestine.